BSGF - Earth Sciences Bulletin 2019, 190, 8

https://doi.org/10.1051/bsgf/2019007

Available online at:
www.bsgf.fr

OPEN ACCESS

Mantle exhumation at magma-poor passive continental margins. Part I. 3D architecture and metasomatic evolution of a fossil exhumed mantle domain (Urdach lherzolite, north-western Pyrenees, France)

Yves Lagabrielle[1,*], Riccardo Asti[1], Serge Fourcade[1], Benjamin Corre[1], Marc Poujol[1], Jessica Uzel[1], Pierre Labaume[2], Camille Clerc[3], Romain Lafay[4], Suzanne Picazo[4] and René Maury[5]

[1] Université de Rennes, CNRS, UMR 6118 Géosciences Rennes, Campus de Beaulieu, 35000 Rennes, France
[2] Université de Montpellier, CNRS, Géosciences Montpellier, 34095 Montpellier, France
[3] LIVE, Université de la Nouvelle-Calédonie, BPR4, 98851 Nouméa cedex, France
[4] Institute of Earth Sciences, University of Lausanne, Géopolis, 1015 Lausanne, Switzerland
[5] Université de Brest, CNRS, UMR 6538 Géosciences Océan, Institut Universitaire Européen de la Mer, place Nicolas-Copernic, 29280 Plouzané, France

Received: 10 January 2019 / Accepted: 10 April 2019

Abstract – In two companion papers, we report the detailed geological and mineralogical study of two emblematic serpentinized ultramafic bodies of the western North Pyrenean Zone (NPZ), the Urdach massif (this paper) and the Saraillé massif (paper 2). The peridotites have been exhumed to lower crustal levels during the Cretaceous rifting period in the future NPZ. They are associated with Mesozoic pre-rift metamorphic sediments and small units of thinned Paleozoic basement that were deformed during the mantle exhumation event. Based on detailed geological cross-sections and microprobe mineralogical analyses, we describe the lithology of the two major extensional fault zones that accommodated: (i) the progressive exhumation of the lherzolites along the Cretaceous basin axis; (ii) the lateral extraction of the continental crust beneath the rift shoulders and; (iii) the decoupling of the pre-rift cover along the Upper Triassic (Keuper) evaporites and clays, allowing its gliding and conservation in the basin center. These two fault zones are the (lower) crust-mantle detachment and the (upper) cover *décollement* located respectively at the crust-mantle boundary and at the base of the detached pre-rift cover. The Urdach peridotites were exposed to the seafloor during the Late Albian and underwent local pervasive carbonation and crystallization of calcite in a network of orthogonal veins (ophicalcites). The carbonated serpentinized peridotites were partly covered by debris-flows carrying fragments of both the ultramafics and Paleozoic crustal rocks now forming the polymictic Urdach breccia. The mantle rocks are involved in a Pyrenean overturned fold together with thin units of crustal mylonites. Continent-derived and mantle-derived fluids that circulated along the Urdach crust-mantle detachment led to the crystallization of abundant metasomatic rocks containing quartz, calcite, Cr-rich chlorites, Cr-rich white micas and pyrite. Two samples of metasomatized material from the crust-mantle detachment yielded in situ zircon U/Pb ages of 112.9 ± 1.6 Ma and 109.4 ± 1.2 Ma, thus confirming the Late Albian age of the metasomatic event. The cover *décollement* is a 30-m thick fault zone which also includes metasomatic rocks of greenschist facies, such as serpentine-calcite association and listvenites, indicating large-scale fluid-rock interactions implying both ultramafic and continental material. The lowermost pre-rift cover is generally missing along the cover *décollement* due to tectonic disruption during mantle exhumation and continental crust elision. Locally, metasomatized and strongly tectonized Triassic remnants are found as witnesses of the sole at the base of the detached pre-rift cover. We also report the discovery of a spherulitic alkaline lava flow emplaced over the exhumed mantle. These data collectively allow to propose a reconstruction of the architecture and fluid-rock interaction history of the distal domain of the upper Cretaceous northern Iberia margin now inverted in the NPZ.

*Corresponding author: yves.lagabrielle@univ-rennes1.fr

Keywords: North Pyrenean Zone / Urdach / mantle exhumation / fluid-rock interactions / listvenites / greenschist facies / detachment faults / Late Cretaceous

Résumé – Exhumation du manteau au pied des marges passives pauvres en magma. Partie 1. Architecture 3D et évolution métasomatique du domaine fossile à manteau exhumé (lherzolite d'Urdach, Pyrénées NW, France). Dans deux articles compagnons, nous décrivons la géologie et la minéralogie de deux massifs de péridotites serpentinisées représentatifs de la Zone Nord-Pyrénéenne (ZNP) occidentale, le massif d'Urdach (cet article) et le massif du Saraillé (article 2). Les péridotites ont été portées vers les niveaux crustaux supérieurs durant l'épisode de rifting pyrénéen crétacé qui a affecté la future ZNP. Elles sont associées à des sédiments métamorphiques pré-rift et à des lambeaux de croûte Paléozoïque déformée durant l'exhumation. En s'appuyant sur des descriptions de coupes géologiques et des analyses de minéraux à la microsonde, nous précisons la lithologie de deux failles extensives majeures qui ont permis : (i) la remontée des lherzolites sous l'axe du bassin ; (ii) l'extraction latérale de la croûte continentale sous les bordures du rift et ; (iii) le découplage et le glissement de la couverture pré-rift le long des évaporites et argiles du Keuper. Ces deux zones de faille sont le détachement croûte-manteau (inférieur) et le décollement de couverture (supérieur) situés respectivement à la limite croûte-manteau et à la base de de la série pré-rift glissée. Les péridotites d'Urdach ont été mises à l'affleurement sur le fond marin où elles ont subi une carbonatation interne partielle accompagnée de cristallisation de calcite dans un réseau de veines orthogonales (ophicalcites). Les serpentinites ont été recouvertes partiellement par la brèche d'Urdach formée d'écoulements de débris ultramafiques et paléozoïques. Les roches du manteau sont engagées avec de minces lentilles de mylonites crustales dans un pli deversé vers l'ouest. Des fluides d'origine mantellique et continentale ont circulé le long du détachement croûte-manteau et ont permis la cristallisation de roches métasomatiques renfermant : quartz, calcite, chlorite et mica riches en Cr, et pyrite. Deux échantillons de ces roches métasomatiques ont fourni des âges U/Pb in situ sur zircons de 112.9 ± 1.6 Ma et 109.4 ± 1.2 Ma confirmant ainsi l'âge Albien supérieur de cet événement métasomatique. Le décollement de couverture renferme aussi des roches métasomatiques (associations calcite-serpentine et listvénites), témoignant d'échanges fluide-roche à grande échelle à partir de matériel mantellique et crustal. La base de la couverture pré-rift a subi une troncature basale lors de l'exhumation du manteau et des résidus triasiques très déformés sont présents à la base de la série pré-rift décollée. Nous avons également découvert une coulée de lave sphérulitique alcaline mise en place sur le manteau exhumé. Cet ensemble de données sur le massif d'Urdach permet de proposer une reconstitution au Crétacé supérieur de l'histoire des fluides et de l'architecture du domaine distal de la marge nord ibérique aujourd'hui inversée dans la ZNP.

Mots clés : zone Nord Pyrénéenne / Urdach / exhumation du manteau / interactions fluide-roche / listvénites / faciès schistes verts / faille de détachement / Crétacé moyen-supérieur

1 Introduction

The architecture of magma-poor passive continental margins is now classically viewed as a succession of three structural domains, namely from continent oceanward: the proximal, necking and distal domains (Péron-Pinvidic and Osmundsen, 2016, and references within). The proximal domain is weakly thinned and displays the thicker crust (25–30 km). The necking domain concentrates crustal stretching accommodated by high-angle normal faulting. The distal domain is characterized by high-displacement, low-angle faults that allow the crust to thin drastically down to 10 km thickness and less (hyper-thinned crust). Complete excision of the continental crust and subsequent unroofing of the subcontinental mantle lithosphere to the seafloor locally occurs in tectonic windows opened in the distal domain. These latter processes lead to a region referred to as the exhumed mantle domain hereafter.

Distal domains of current passive margins lie at abyssal depths with difficult access and only a few exhumed mantle domains could be investigated worldwide through drilling and dredging: the North Atlantic conjugate margins (Boillot *et al.*, 1987; Tucholke *et al.*, 2007; Péron-Pinvidic and Manatschal, 2009, and references within), the South Australian margin (Beslier *et al.*, 2004; Gillard *et al.*, 2015), and the South China Sea margins (IODP Legs 367 and 368, Larsen *et al.*, 2018). During the last 30 years, considerable academic efforts have been carried out in order to collect samples from the conjugate Iberia-Newfoundland margins with the aim to unravel the tectonic and metasomatic evolution of the hyperthinned crust and exhumed subcontinental mantle during continental breakup (i.e. Pérez-Gussinyé *et al.*, 2006; Reston, 2009a, 2009b; Pérez-Gussinyé, 2013; Sutra *et al.*, 2013). Despite these efforts, our knowledge of the geological architecture of the exhumed mantle domain, and consequently, our understanding of the processes that enable subcontinental peridotites exhumation and their unroofing to the seafloor, remains relatively poor. To bridge this gap in knowledge, geologists investigate inverted paleo-passive margins now incorporated into orogenic belts. Despite strong imprint of collisional deformation, distal passive margin domains can be directly

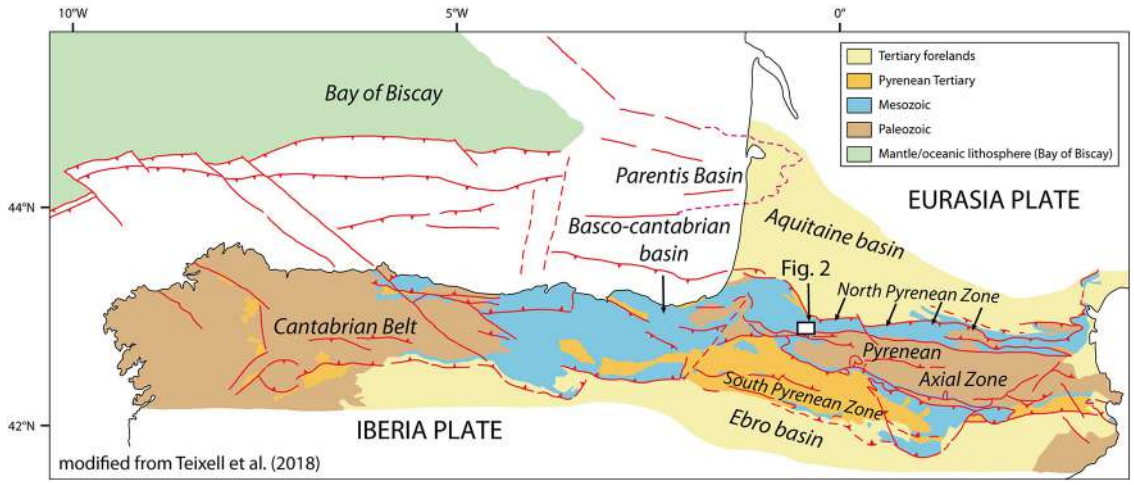

Fig. 1. Simplified structural map of the Pyrenean-Cantabrian belt and location of the study area (modified after Teixell *et al.*, 2018).
Fig. 1. *Carte simplifiée de la chaîne Pyrénéo-cantabrique et localisation de la zone étudiée (modifiée d'après Teixell* et al.*, 2018).*

sampled in some internal units of Alpine or Caledonian orogens (i.e. Lemoine *et al.*, 1987; Manatschal and Nievergelt, 1997; Manatschal, 2004; Marroni and Pandolfi, 2007; Wrobel-Daveau *et al.*, 2010; Andersen *et al.*, 2012; Chew and van Staal, 2014; Mohn *et al.*, 2012; Jakob *et al.*, 2019). These field analogs represent unique geological laboratories enabling direct study of the architecture, modes of deformation and plumbing systems of the deepest portions of continental passive margins.

In two companion papers, we describe and discuss the geology of two remarkable field analogs located in the Pyrenean belt, the Urdach and Saraillé massifs, where portions of inverted distal domains of magma-poor continental passive margins can be investigated. The present article focuses on the structure of the Urdach lherzolite body and associated continental units, in the northwestern Pyrenees. Based on new detailed mapping, we first describe the structures deriving from the Pyrenean collision and we show that they have not completely altered the original rifting architecture. This allows us to constrain the structure and the metasomatic evolution of the fault zones along which the subcontinental mantle reached shallow crustal levels before final unroofing to the sea-floor of Cretaceous basins opened along the diverging Eurasian-Iberian plate boundary. A tight sampling of all lithologies exposed around the Urdach lherzolite allows us to propose a 3D-reconstruction of a portion of the landscape that composed the distal domain of the north Iberia margin in the mid-Cretaceous times. We also provide the first mineralogical analyses of the metasomatic assemblages composing most of the fault rocks completed by two in-situ U/Pb zircon dating. These assemblages are the witnesses of the fluid-rock interactions operating in the exhumed mantle domain during the complete removal of the continental crust. Through these geological and hydrothermal reconstructions, we aim at providing a new set of geological data that may be used as field references for remote distal domains of current passive continental margins.

2 Geological setting

2.1 The Pyrenees and the lherzolite bodies in the North Pyrenean Zone (NPZ) (Fig. 1)

The Pyrenean belt is a double-verging chain resulting from the collision of the southern and northern margins of the Eurasian and Iberian plates respectively (Choukroune and ECORS team, 1989; Roure *et al.*, 1989; Muñoz, 1992; Vergés *et al.*, 1995; Teixell, 1998; Mouthereau *et al.*, 2014; Teixell *et al.*, 2016, 2018; Chevrot *et al.*, 2018). Shortening in the Pyrenees did not exceed 150 km, but was sufficient to allow the distal portions of the inverted Iberia margin to be uplifted and to be now exposed along the northern flank of the belt (Lagabrielle and Bodinier, 2008; Jammes *et al.*, 2009; Lagabrielle *et al.*, 2010; Masini *et al.*, 2014; Tugend *et al.*, 2014, Teixell *et al.*, 2016, 2018; Corre *et al.*, 2016).

The E-W-trending Pyrenean thrust-and-fold belt consists of a core of Paleozoic rocks forming the elevated Axial Zone, bounded to the south by the South Pyrenean Zone (SPZ) mostly formed by detached Mesozoic thrust-sheets comprising synorogenic Upper Cretaceous-Tertiary flysch and molasse sediments, and to the north by the North Pyrenean Zone (NPZ), a narrow belt of Mesozoic sediments containing remnants of subcontinental mantle lherzolites (Monchoux, 1970; Vielzeuf and Kornprobst, 1984; Fabriès *et al.*, 1991, 1998). The NPZ is bounded to the south by the E-W-trending North Pyrenean Fault (NPF). Continental rifting in the Pyrenean realm occurred synchronously with oceanic spreading in the Bay of Biscay, in relation with the counterclockwise rotation of the Iberia plate during the mid-Cretaceous (Le Pichon *et al.*, 1970; Choukroune and Mattauer, 1978; Olivet, 1996; Sibuet *et al.*, 2004; Vissers and Meijer, 2012). Rifting leading to crustal separation was accompanied by the ascent of subcontinental lithospheric mantle in the axis of the future NPZ (Vielzeuf and Kornprobst 1984; Lagabrielle and Bodinier, 2008 and references within). Finally, the collision of the northern Iberia

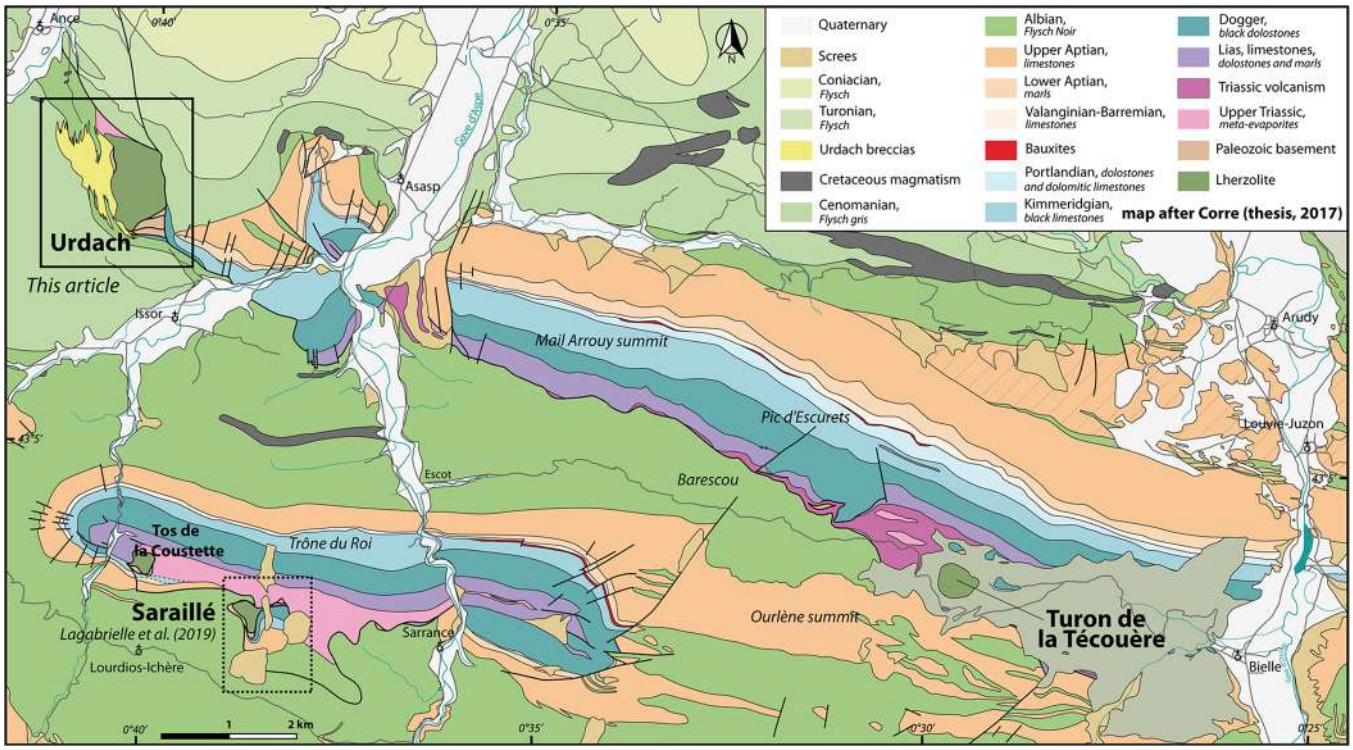

Fig. 2. Geological map of the "Chainons Béarnais" (Corre, 2017) and location of the Saraillé and Urdach lherzolite bodies.
Fig. 2. *Carte géologique des « Chainons Béarnais » (Corre, 2017) et situation des massifs du Saraillé et d'Urdach.*

and southern Eurasian plate margins occurred during the Late Cretaceous-Tertiary (Muñoz, 1992; Roure and Choukroune, 1998; Teixell, 1998; Vergés and Garcia-Senz, 2001; Mouthereau *et al.*, 2014; Teixell *et al.*, 2016, 2018).

Based on their geological setting, the small Pyrenean mantle bodies of the NPZ have been classified in two types (Lagabrielle *et al.*, 2010). In the S-Type (sedimentary type), the lherzolite bodies are included within clastic sedimentary formations. Emblematic examples are the Lherz body in the Aulus Cretaceous basin and the Bestiac-Prades bodies in the Tarascon basin (Lagabrielle *et al.*, 2016; Saint Blanquat *et al.*, 2016). In the T-type (tectonic type), the lherzolite bodies exhibit tectonic relationships with the surrounding Mesozoic formations of the NPZ. They are most often associated with cataclastic Triassic rocks and with thin tectonic lenses of Paleozoic rocks.

Exhumation of subcontinental mantle undoubtedly appears as an important mechanism accompanying the processes of extreme thinning of the continental crust during plate separation all along the Pyrenean realm (Lagabrielle and Bodinier, 2008; Jammes *et al.*, 2009; Lagabrielle *et al.*, 2010; Masini *et al.*, 2014; Clerc *et al.*, 2016; DeFelipe *et al.*, 2017). Correlation between metamorphic and chronological data have demonstrated that extensional deformation of the pre-rift Mesozoic sequences and thinning of the continental basement of the NPZ occurred under low pressure and high temperature (LP-HT) conditions (Golberg and Leyreloup, 1990; Clerc *et al.*, 2015). In recent models based on geological observations, rifting in the future NPZ involves the lateral extraction of the ductilely thinned and boudinaged Variscan basement under a detached Mesozoic pre-rift cover mechanically decoupled from that basement by means of clays and evaporites of Late Triassic age (Keuper deposits) (Clerc and Lagabrielle, 2014; Clerc *et al.*, 2016; Lagabrielle *et al.*, 2016). These models emphasize the early tectonic juxtaposition of exhumed mantle rocks against the allochthonous pre-rift sediments. They also imply a tectonic behaviour of the continental crust with a necking domain characterized by smooth-slope conjugate margins and a distal domain characterized by ductile stretching (Corre *et al.*, 2016; Lagabrielle *et al.*, 2019). Finally, these models are consistent with paleomargin architectures reconstructed by Teixell et al. (2016, 2018) which constrast with former reconstructions from the western NPZ (Mauléon basin) by the absence of extensional allochthons in the distal domain (Jammes *et al.*, 2009; Masini *et al.*, 2014).

2.2 The Chaînons Béarnais and their four mantle bodies (Fig. 2)

The Chaînons Béarnais range exposes the Mesozoic pre-rift and syn-rift sediments of the western NPZ. In its western area, it consists of three E-W-trending and parallel thrust-fold structures: the Mail Arrouy monocline, and the Sarrance and Layens anticlines, bounded by north- and south-verging, post-Cenomanian thrust faults (Casteras *et al.*, 1970) (Fig. 2). To the west, the structures plunge westward in the Mauléon basin. The stratigraphic sequence of the Chaînons Béarnais represents the original cover of the northern Iberian margin and consists of basal brecciated

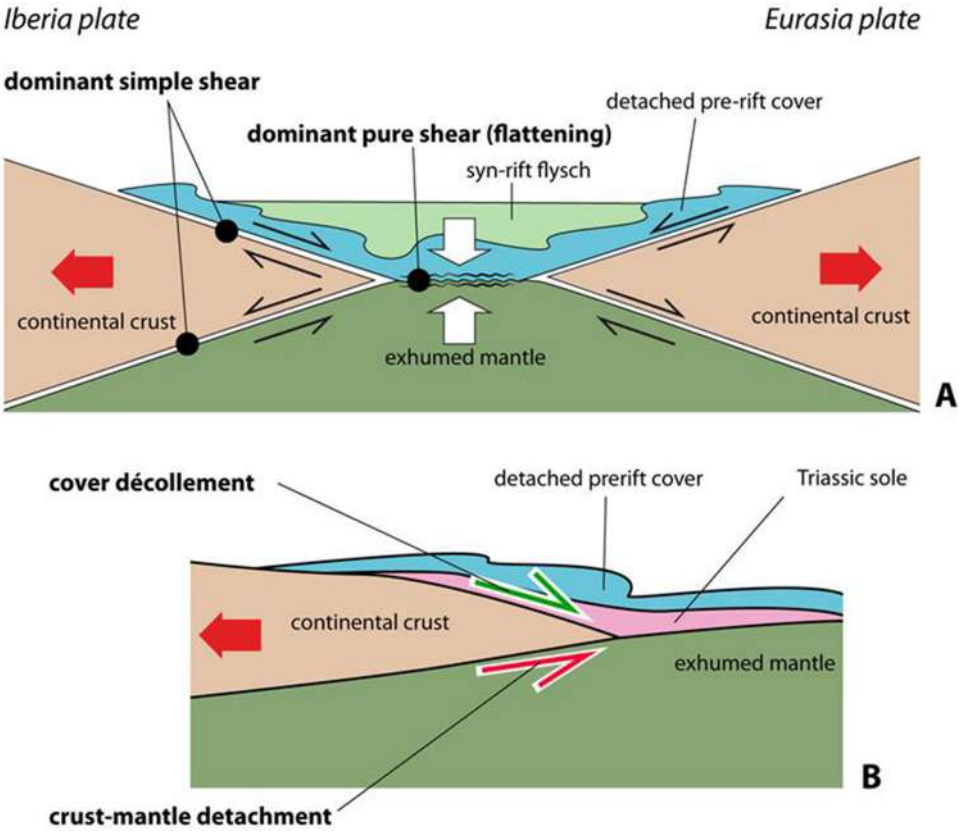

Fig. 3. Cartoons illustrating some tectonic aspects of idealized passive margins with mantle exhumation and denudation. A. Location of the domains dominated respectively by simple and pure shear deformation modes. B. Location of the crust-mantle detachement and cover *décollement* in the distal margin domain.

Fig. 3. *Schémas des éléments tectoniques caractéristiques dans une marge passive distale à manteau exhumé. A. Répartition des modes de déformation en cisaillements simple et pur. B. Position du détachement croûte-manteau et du décollement de couverture dans la marge distale.*

Upper Triassic sediments (Keuper facies) and hypo-volcanic basaltic rocks (ophites), followed by Mesozoic platform carbonates (Canérot *et al.*, 1978; Canérot and Delavaux, 1986). This sequence is tectonically disconnected from its former Paleozoic basement known only as very small tectonic slices or as breccia fragments. The platform carbonates comprise a succession of Jurassic to Upper Aptian metamorphic limestones, dolomites and subordinate marls forming the current main reliefs. This platform succession terminates with a thick (300–400 m) layer of Upper Aptian limestones (Urgonian facies), and is followed by a thick sequence of Albian to Cenomanian-Turonian flysch deposits (e.g. Debroas, 1978; Debroas *et al.*, 2010; Canérot, 2017a, 2017b and references within) preserved within the synclines and marking the main rifting stage. The Chaînons Béarnais range hosts four main lherzolite bodies: the Saraillé and Tos de la Coustette bodies in the southern flank of the Sarrance anticline, the Urdach body at the western tip of the Mail Arrouy anticline, and the Turon de la Técouère body in the strongly tectonized zone of Benou, along the southern border of the Mail-Arrouy thrust structure (Fig. 2). The Saraillé lherzolites are highly serpentinized and lie in tectonic contact with thin Paleozoic lenses and with ductilely deformed Mesozoic carbonates bearing LP-HT metamorphic paragenesis (Fortané *et al.*, 1986; Thiébault *et al.*, 1992; Corre *et al.*, 2016). The Saraillé mantle rocks represent the emblematic example of the T-type lherzolites (Lagabrielle *et al.*, 2010; Corre *et al.*, 2016). The Urdach lherzolites belong to both the T-type and S-type (Jammes *et al.*, 2009; Debroas *et al.*, 2010; Lagabrielle *et al.*, 2010; DeFelipe *et al.*, 2017). They display a more complex setting involving lenses of Paleozoic rocks and sedimentary crustal-mantle breccias as reported in the following sections.

2.3 Definition of the crust-mantle detachment and cover *décollement* (Fig. 3)

Remnants of two types of low-angle shear zones that accommodated the extension of the distal domain of the Iberia passive margin during the mid-Cretaceous are exposed in both the Urdach and the Saraillé massifs. The deepest shear zone separates the ultramafic mantle rocks from strongly thinned continental Paleozoic rocks and is named the crust-mantle detachment hereafter. The shallowest one marks the boundary between the base of the detached pre-rift Mesozoic metasedimentary cover and either mantle lherzolites or

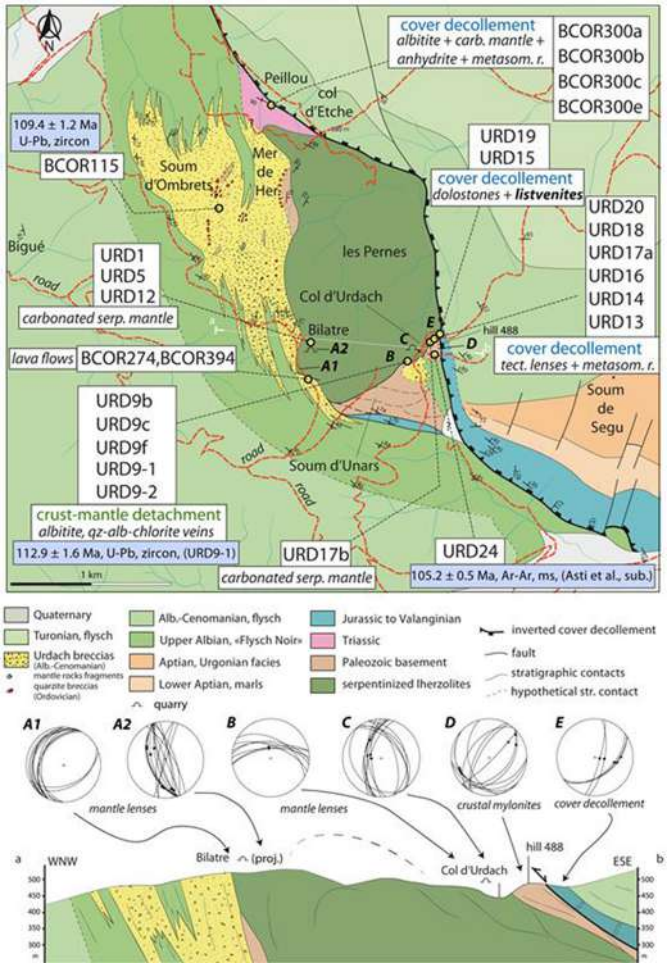

Fig. 4. Detailed geological map of the Urdach massif (Corre, 2017) and corresponding geological cross-section ab. Location of the studied samples. Stereonets A1, A2, B and C show the orientation of shear zones separating tectonic lenses in the lenticular layer of the Urdach mantle (dots are striae trends). Stereonet D shows the orientation of shear zones and striae in the felsic mylonites of hill 488 (Asti *et al.*, 2019). Stereonet E shows the orientation of normal faults and associated striae in the "ball trap" section (Urdach cover *décollement*) (see faults on Fig. 10).
Fig. 4. *Carte détaillée du massif d'Urdach (Corre, 2017) et coupe ab. Stéréogrammes A1, A2, B, C et D repérés sur la carte.*

continental basement rocks. It is named the cover *décollement* hereafter and corresponds to a thick deformation zone (some meters to tens of meters thick) that was the locus of significant metasomatic crystallizations involving notably Triassic fluids (Corre *et al.*, 2016). The crust-mantle detachment fault zone is better studied in the Saraillé massif (see companion paper Lagabrielle *et al.*, 2019). It is composed of a basal 20–50 m thick layer of sheared serpentinites named the lenticular layer, followed by a 10-m thick damage zone. The lenticular layer consists of ultramafic symmetrical tectonic lenses, a few meters long, separated by anastamosing serpentine-rich shear zones. The damage zone consists of an assemblage of centimeter-sized symmetrical lenses of a soft, talc-rich, sheared material, separated by conjugate shear zones. In the Saraillé massif, this layer is the locus of local carbonation of the mantle rocks and represents an important pathway for exhumation-related metasomatic fluids (see companion paper Lagabrielle *et al.*, 2019).

3 Anatomy of the crust-mantle detachment and cover *décollement* in the Urdach massif: structure and mineralogy

3.1 Geology of the Urdach massif (Fig. 4)

3.1.1 Overview of former interpretations

The Urdach mantle body lies at the western termination of the Mail Arrouy thrust monocline, between Col d'Urdach and Col d'Etche, and is the easternmost basement exposure of the Mauléon basin (Canérot, 2017a, 2017b). This 1.5-km long lherzolite body is well known for its association with sedimentary breccias of Late Albian age, named the Urdach breccia hereafter (Casteras *et al.*, 1970; Roux, 1983; Debroas *et al.*, 2010). The Urdach breccia are polymictic debris flows deposits composed of centimeter- to meter-sized clasts of talcified and serpentinized mantle rocks mixed with fragments of dominant ortho- and para-derived

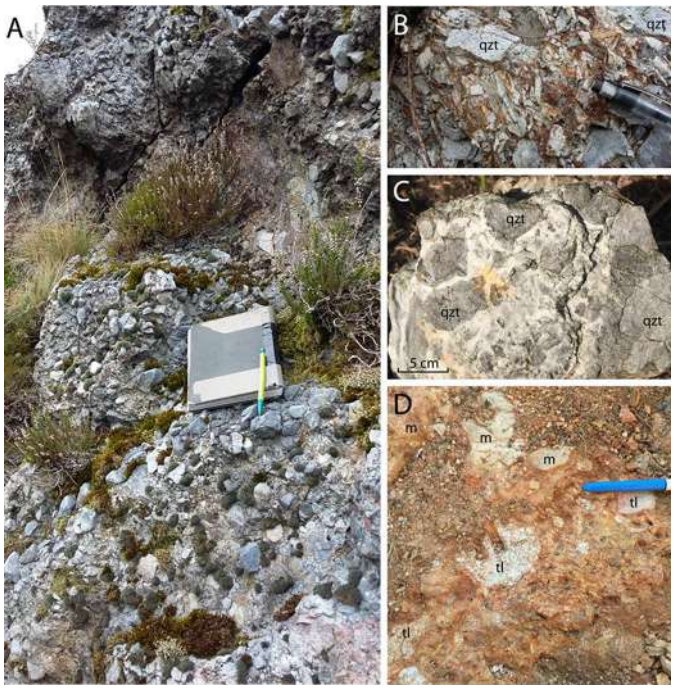

Fig. 5. Photographs showing some typical field aspect of the Urdach breccia. A. General aspect. B. A layer composed of numerous angular clasts of quartzite mylonite. C. Typical aspect of the breccia in the Mer de Her area. Quartzite clasts are cemented by hydrothermal quartz with fluid inclusions of Triassic origin (Nteme, 2017). D. Aspect of the Urdach polymictic breccia near Bilatre (qzt: Ordovician (?) quartzites; m: mylonitic Paleozoic basement; tl: talcified lherzolites).
Fig. 5. *Photographies montrant quelques aspects typiques des brèches d'Urdach.*

mylonitic Paleozoic rocks and subordinate Mesozoic metasediments (Fig. 5 and Fig. S1 in Supplementary Material). The Urdach breccia may be locally up to 1000 m thick and includes large olistoliths of distinct origin: serpentinized lherzolites, Silurian black schists, and Toucasia-bearing Aptian marbles belonging to the original pre-rift cover of the Paleozoic basement (Debroas *et al.*, 2010). The clast sources of the Urdach breccia indicate that juxtaposed units of continental crust and mantle peridotite have been exposed on the floor of the NPZ rift basins during the Late Cretaceous. Exposure of the mantle rocks at the seafloor is consistent with the occurrence of ophicarbonate breccias (ophicalcites) in a quarry located on the western side of the lherzolite body (Bilatre quarry: Jammes *et al.*, 2009; Lagabrielle *et al.*, 2010; Clerc *et al.*, 2014; DeFelipe *et al.*, 2017). Ophicalcites are well known at the interface between ultramafic rocks and seawater along slow-spreading ridges as well as in numerous ophiolites worldwide (e.g. Trommsdorff *et al.*, 1980; Lemoine, 1980; Früh-Green *et al.*, 2003; Boschi *et al.*, 2006a; Lafay *et al.*, 2017).

Three interpretations have been proposed to account for the geological setting of the Urdach lherzolites. They involve:

– emplacement of a large-scale olistolith of composite mantle-crustal basement in the Albian-Cenomanian flyschs (Duée *et al.*, 1984; Fortané *et al.*, 1986);
– mantle denudation along a former N-S Urdach transverse fault scarp zone (Debroas *et al.*, 2010);
– thrusting of a slice of mantle rocks and its cover made of tectono-sedimentary breccia over verticalized Upper Cretaceous flysch strata (Jammes *et al.*, 2009; Lagabrielle *et al.*, 2010).

3.1.2 New data from recent field works

Based on a new detailed geological mapping of the Urdach area, we are now able to update the main characteristics of the lherzolite body and associated lithologies (Fig. 4). These characteristics have been compiled by Asti *et al.* (2019) and can be summarized as follows:

– at various places, the mantle rocks are closely associated with hectometer-sized lenses of intensively sheared Paleozoic rocks, only a few decameter-thick, that lie immediately beneath the Urdach breccia or beneath the pre-rift cover. These lenses are relatively well exposed on the western (Mer de Her), southern (Soum d'Unars) and eastern side (hill 488) of the mantle body and are labelled on Figure 4. The foliation of these crustal lenses always parallels the geological boundary of the adjacent mantle rocks, a major structural characteristic also noticed in the Saraillé massif (Corre *et al.*, 2016; Asti *et al.*, 2019);
– the Urdach breccia and interbedded flysch strata are continuously exposed from Col d'Urdach to Col d'Etche and represent the early sedimentary cover of the peridotites and associated sheared Paleozoic rocks;
– ophicalcites also occur in the walls of a quarry located at Col d'Urdach, at the opposite side of the Bilatre quarry. This implies that a large portion of the peridotites exposed in the Urdach massif derive from a former seafloor composed of unroofed serpentinized mantle rocks associated with exhumed Paleozoic basement material;
– our compilation of dip measurements confirms previous measurements by Debroas *et al.* (2010) and demonstrates that the Urdach breccias and the Albian-Cenomanian flysch strata are in a reverse position along the western side of the mantle body (Fig. 4). This implies that the Mesozoic sediments are involved in a kilometer-scale recumbent fold with the Urdach ultramafic basement in its core (see section ab, Fig. 4);
– the cover *décollement* can be traced between a thin unit of Jurassic marbles and Paleozoic schists along the southern border of the massif south of Soum d'Unars. Eastward, it separates the Urdach serpentinites from the Mesozoic sequence of the Mail Arrouy monocline and is exposed immediately north of the Col d'Urdach. It can be followed northwards to the northern end of the Urdach body, in the site of Peillou, a region of poor exposures, where it separates strongly deformed remnants of Triassic metasediments from the base of the Mail Arrouy flysch sequence (Fig. 4).

3.2 The Urdach crust-mantle detachment

In the Urdach massif, the crust-mantle detachment corresponds to the boundary between the thin Paleozoic lenses and the mantle lherzolites. It can be traced along the

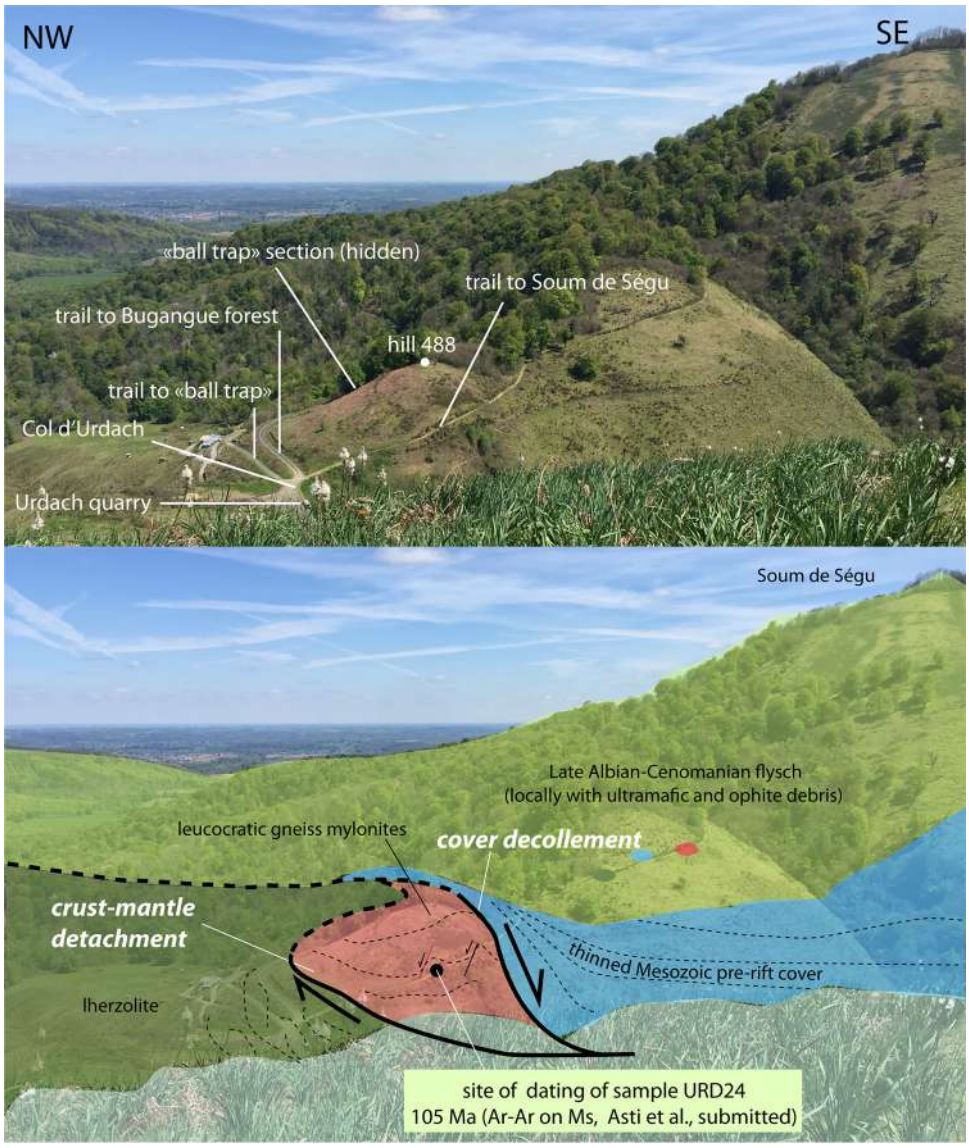

Fig. 6. Geological interpretation of a panoramic view of the Col d'Urdach area taken from the summit of Soum d'Unars looking to the NE. Trails, roads and main fault contacts cited in text are shown.
Fig. 6. *Vue panoramique sur le Col d'Urdach depuis Soum d'Unars. On regarde vers le NE.*

southern and western limits of the lherzolites from Col d'Urdach to Col d'Etche/Peillou. It is relatively well exposed in one single location only, at the site of sample series URD9, immediately west of the Col d'Urdach (Fig. 4) (samples URD9-1, URD9-2 and URDa to f).

3.2.1 The Urdach mantle: tectonic lenses and ophicalcites

Mantle rocks belonging to the uppermost levels of the exhumed mantle can be observed around the Col d'Urdach, in the serpentinite quarry as well as along the scarps of the roads to the Bugangue forest and to the "ball trap" (see 3D view of Fig. 6 for precise location). These outcrops allow critical observation of the strain pattern of the crust-mantle detachment at the final stages of the exhumation process. In the Col d'Urdach quarry, anastomozing shear zones are observed at different scales, defining a clear lenticular fabric (Fig. 7A, B). The conjugate extensional shear zones delineate a series of tectonic lenses, a few meters wide, and multiple phacoids of smaller size with evidence of syn-kinematic growth of fibrous serpentine and calcite (Fig. 7D). This lens-shaped tectonic fabric typically corresponds to the fabric of the lenticular layer as defined in the uppermost-serpentinized mantle of the nearby Saraillé massif (see companion paper, Lagabrielle *et al.*, 2019). On the floor of the southern part of the Col d'Urdach quarry as well as along its northern wall, some shear zones and conjugate joints are invaded by thin veins of calcite, giving the rock the texture of typical ophicalcites (Fig. 8A). A later tectonic brecciation along some shear zones led to the individualization of elongated lenses composed of centime-

Fig. 7. The lenticular layer of the crust-mantle detachment exposed at Col d'Urdach and close to Bilatre (see Fig. 4 for location). A. Shear bands with white layers of serpentine minerals above the "ball trap". B. Tectonic lenses in the Col d'Urdach quarry. C. Gouge and tectonic breccia along a subvertical fault zone in the Col d'Urdach quarry. D. Calcite crystallization on a fault surface (Bilatre quarry entry). E. Fault zone in the Bilatre quarry. F. Tip of a tectonic lens showing the transition from carbonate-free to carbonated serpentinized mantle (Bilatre quarry). G. Ophicalcite of the Bilatre quarry showing at least two generation of calcite veins (V1, V2). H. Tectonic fabric in the lenticular layer enhanced by anatomozed calcite veins (loose block near Bilatre). I. Phacoidal fabric in a large olistolith of the Urdach breccia (Bilatre).

Fig. 7. *La zone lenticulaire du détachement croûte-manteau au Col d'Urdach et à Bilatre (vues de terrain).*

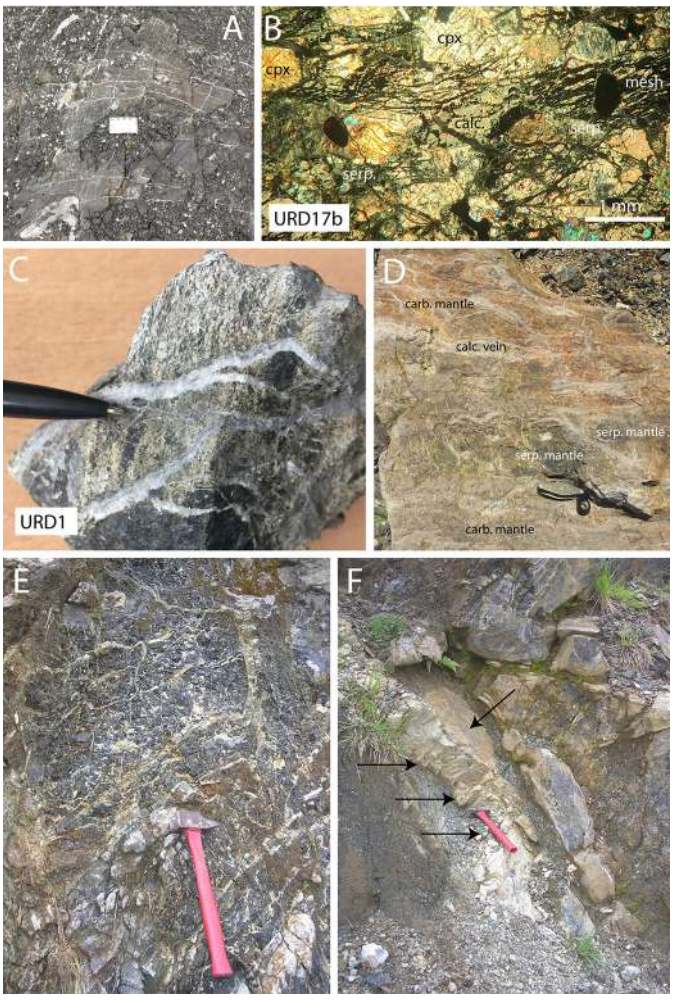

Fig. 8. Ophicalcites at Col d'Urdach and at Bilatre. Field and microscopic aspect. A. Undeformed ophicalcites on the floor of the Col d'Urdach quarry. B. Slightly carbonated mantle lherzolite at the Col d'Urdach "ball trap" section. Note the mesh texture (cpx.: clinopyroxene; serp.: serpentine; calc.: calcite). C. Calcite veining in ophicalcite sample URD1 from the Urdach quarry. D. Alternating carbonated and carbonate-free layers of serpentinized mantle (Bilatre quarry). E. Multidirectional network of calcite veins (Bilatre quarry). F. Albitite dike (arrows) at the Bilatre quarry in 2007. This outcrops does not exist anymore due to oversampling.

Fig. 8. *Les ophicalcites du Col d'Urdach et de Bilatre (vues de terrain et aspects microscopiques).*

ter- to millimeter-sized ultramafic clasts surrounded by serpentinite gouges (Fig. 7C, E). Unfortunately, it was not possible to determine whether such late brecciation and development of cataclastic shear bands relates to the pre-inversion history of the orogen or to its Cenozoic contractional evolution.

The lenticular fabric is also observed on the western side of the mantle body, in the Bilatre quarry (Fig. 7F, G, H). The anastomozing shear zones separating the serpentinite lenses are composed of millimeter-thick layers of foliated serpentine locally invaded by multiple thin calcite layers (Fig. 8C, D). Multi-layered calcite precipitates develop as well in orthogonal fractures cross-cutting the lenses and form by place a dense vein network (Fig. 7G). The widest multi-layered calcite veins may be one decimeter thick. Evidence of syn-kinematic calcite crystallization is observed in some places with calcite fibers lying on serpentine fault surfaces (Fig. 7D). The densest network of calcite veins is observed in the center of the quarry. Here, the rock exhibits the typical aspect of ophicalcites as described in the reference site of the Ligurian ophiolites (e.g. Treves and Harper, 1994). Occasionally, in the Bilatre quarry, the mantle rocks display a layered aspect due to alternating carbonate-rich and foliated serpentine beds (Fig. 8D). The carbonate-rich layers

correspond to deeply carbonated serpentinites and display a light-pink or orange color, contrasting with the dark green color of the surrounding carbonate-free serpentinized lherzolites. We sampled the serpentinized mantle and the ophicalcites of the Bilatre quarry (samplesURD4, URD5 and URD1, URD12, respectively) in order to better constrain the evolution of the carbonation process in the exhumed mantle (see location of samples in Fig. 4).

Results of microstructural measurements (dips of foliation planes and associated striaes) in the lenticular layer are reported in Figure 4. We are well aware that, owing to subsequent deformation during the Pyrenean orogeny, any attempt to precisely reconstruct the geometry of exhumation-related tectonic markers is hazardous. Nevertheless, measurements show that at the eastern and western sides of the Urdach body (Col d'Urdach area and the Bilatre quarry), the borders of the mantle lenses are dipping at high angle, a geometry consistent with the attitude of the boundary of the mantle body and with the attitude of the edges of the continental unit at hill 488 and at Mer de Her (Fig. S1, Supplementary Material) (Asti *et al.*, 2019). Striae and fibers measured on the planes of the serpentinized mantle lenses show E-W and N-S direction families (see stereonets in Fig. 4). The latter family can be assigned to the compressional stage of the Pyrenean orogeny. The E-W family is consistent with the direction of calcite fibers measured along the normal fault that separates the Urdach mantle rocks from the pre-rift cover along the cover *décollement* (see next section). This direction is consistent with the trends of striae lying on the foliation planes of the crustal mylonites at hill 488. All these directions indicate extension in the E-W to NE–SW quadrants and can be attributed to the exhumation phase, keeping in mind that unknown amount of further rotation occurred during the Pyrenean compression.

3.2.2 The Urdach crust-mantle detachment: field data

The crust-mantle detachment is rarely exposed in the Urdach area. Relationships between felsic rocks and the Urdach lherzolites can be investigated in a few sites only such as at hill 488, between Mer de Her and Col d'Etche and on the east flank of Soum d'Unars (Fig. 4). In the following subsections (1 to 3), we describe the main geological features observed at each of these sites:

– the contact between the Urdach mantle rocks and a tectonic lens of mylonitic Paleozoic leucocratic gneisses can be traced at the base of the hill 488 (site of sample URD24 dating, Asti *et al.*, 2019) (Fig.6). This contact is not directly exposed. A trail that runs E-W from Col d'Urdach to Soum de Ségu crosses the contact but no continuous outcrop could be observed that would allow to study in detail the crust-mantle relationships here;
– North-west of the Urdach massif, in the Mer de Her area, cataclastic breccias are abundant as loose blocks, close to the lens of Silurian black schists welded against the western border of the lherzolites. Unfortunately, the contact between the schists and the lherzolites is not exposed. The N-S oriented foliation of the schists dips at high angle, parallel to the western edge of the mantle rocks (Fig. S1C, in Supplementary Material). In the vicinity of the schists, numerous blocks of monomictic tectonic breccias composed of clasts of quartzite, probably of Ordovician age, are observed. The clasts are welded by two generations of quartz cement and most of them are cross-cut by an early generation of quartz veins. Analyses of fluid inclusions in the quartz veins and cement have been performed in the breccias from these outcrops (Nteme, 2017) (Fig. S1D, E, F in Supplementary Material);
– a contact between the serpentinized mantle and felsic rocks is exposed along an abandoned trail, east of the Soum d'Unars summit and immediately west of the Col d'Urdach quarry (Fig. 4). An E-W vertical fault separates the serpentinized lherzolites from a light-colored chloritized felsic rock (sample URD9-1, Fig. 9A) reminiscent of the Cretaceous albitite dikes cross-cutting the Urdach mantle (Pin *et al.*, 2001, 2006) rather than of Paleozoic lithologies. This sample was selected for U-Pb dating (see section V).

Fig. 9. Field aspect and metasomatic rocks of the crust-mantle detachment at the site of sample URD9-1. A. Contact between mantle rocks and the albitite-like sample URD9-1. B. Chlorite-albite assemblage with a granitoid aspect. C. Layered quartz-chlorite-micas vein border. The green micas are Cr-rich muscovites (fuchsites). D. Quartz and iron oxide association in a vein (loose block at Soum d'Unars). E. Chlorite-albite assemblage with a granitoid aspect. F. Interior of quartz vein showing ghosts of centimeter-sized pyrites now replaced by limonite.

Fig. 9. *Les roches métasomatiques sur le site de l'échantillon URD9-1 (vues de terrain).*

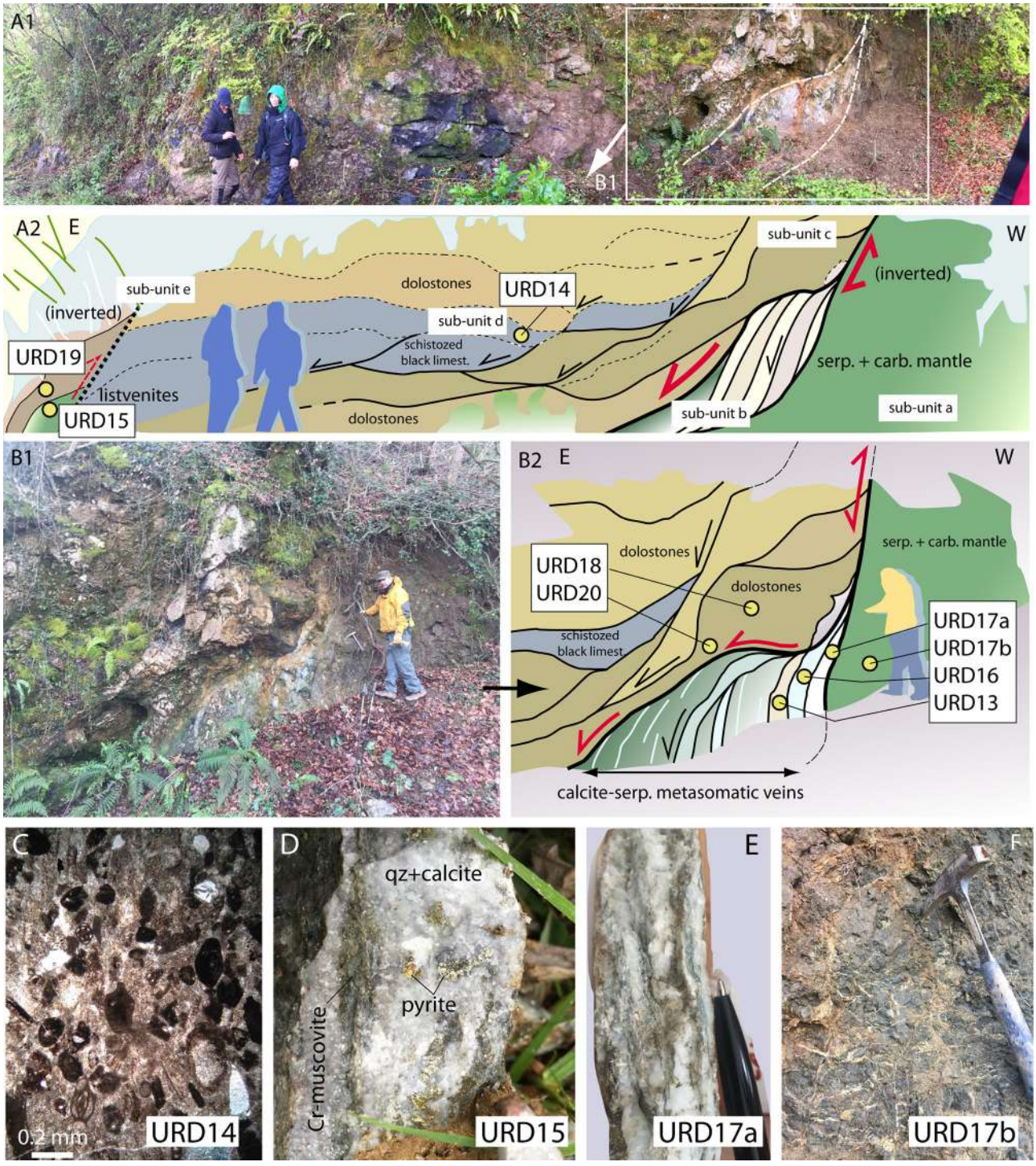

Fig. 10. The cover *décollement* at the "ball trap" site. A1 and A2. Interpreted geological cross-section. B1 and B2. Detail of the contact between the pre-rift cover and the Urdach mantle rocks with location of samples described in text. Note the presence of metasomatic veins (tension gashes: close up in E). C. Microscopic view of sample URD14 containing Liassic microfauna (determination J. Canérot). D. The URD15 listvenite. E. Alternating calcite and serpentine thin layers in a metasomatic vein (sample URD17a). F. Ophicalcites in the "ball trap" cover *décollement* foot wall (sample URD17b). Location of samples in shown in A2 and B2.
Fig. 10. *Le décollement de couverture au site du « ball trap ».*

Close to this albitite-like rock, we observe a poorly deformed, light-colored coarse-grained rock composed of plurimillimeter-sized green euhedral chlorite flakes in a a feldspar-rich groundmass (Fig. 9B, E). This rock, that mimics a granitoid, is observed along a distance of 10 m from the fault contact. It is crosscut by vertical fault zones with a core of strongly foliated green chloritites and light-green mica-chlorite-rich rocks (sample URD9-2) associat-

ed with quartz veins, a few decimeters thick (samples URD9-2, URD9-b, URD9-c and URD9-f, Fig. 9C). The core of the quartz veins displays pseudomorphs of centimeter sized pyrite crystals now changed into orange alteration products, probably limonite, that developed in abundance parallel to the vein limits (samples URD9-a and URD9-d) (Fig. 9F).

3.2.3 The Urdach breccia

We carefully examined the Urdach breccia in order to find out components that would originate directly from the disaggregation of fault rocks belonging to the crust-mantle detachment. The largest ultramafic meter-sized blocks exposed along the road west of Bilatre show a phacoidal fabric indicating that they derive from the mantle lenticular layer (Fig. 7I). In addition, decimeter-sized lherzolite blocks observed inside the breccia between Bilatre and Soum d'Ombrets display a typical pink color and are intensively talcified (Fig. 5D). Talcification may have occurred in the damage zone, as observed in the Saraillé massif, and before sedimentary reworking. Among the largely dominant crustal mylonites sampled in the Urdach breccia (see Asti *et al.*, 2019, for more details), we found one sample of a chloritite (sample BCOR115). In the Urdach area, chloritites are known only at the contacts of the corundum-bearing albitite dikes (Pin *et al.*, 2001, 2006; Monchoux *et al.*, 2006) and at site of sample URD9-2. Sample BCOR115 has been the target of in situ zircon U/Pb dating (see section V).

3.2.4 Microscopic study and mineralogy

This section appears in the text file of Supplementary Material.

3.3 The Urdach cover *décollement*

3.3.1 The Urdach cover *décollement* at the "ball trap" section

The cover *décollement* is exposed immediately north-east of the Col d'Urdach along the road that enters the Bugangue forest, immediately above the "ball trap" site (Fig. 6). The fault zone is more than 30 m wide and involves various rock-types representing deformed original protoliths as well as newly-formed metasomatic rocks and veins. The reconstructed succession consists of five sub-units as follows, from S to N (Fig. 10).

3.3.1.1 Sub-unit a (Fig. 10A2, B2)

The dark Urdach lherzolites are deeply serpentinized and display an orthogonal network of thin and elongated calcite veins that cross-cut each other regularly every 5–10 cm (sample URD17b, Fig. 10D). There is no evidence of post-veining deformation some meters away from the main fault surface. Locally, the serpentinites have a red color similar to some ophicalcites in Liguria and in the Alps (e.g. Bracco and Totalp ophiolites, Weissert and Bernoulli, 1985).

The lherzolites are separated from the Mesozoic sediments by a major fault surface oriented N30 to N15 and dipping to the north at high angle (80°) (stereonet E, Fig. 4). When approaching the fault plane, the ophicalcites are progressively sheared. Along the fault surface itself, the calcite veins are all parallel and separated by very thin septae of strongly sheared serpentinites. C/S relationships of sigmoidal lenses in the fault plane indicate a reverse sense of shear. This motion corresponds to the tectonic inversion of a previous extensional fault as argued below.

3.3.1.2 Sub-unit b (Fig. 10A2, B2)

Immediately north of the fault surface, the basal part of the exposure consists of a series of elongated calcite veins, a few centimeter-thick, alternating with laminated serpentine- and chlorite-rich septae oriented N10 and dipping to the north at high angle (70°) (Fig. 10B2). These calcite veins correspond to a series of parallel sigmoidal tension gashes indicating a normal sense of shear along the fault. Striations on the calcite planes dip at high angle (stereonet E, Fig. 4). Samples URD17a (Fig. 10D) and URD16 have been collected in two distinct calcite veins separated by a distance of less than one meter. A few decimeters north of sample URD16, the calcite veins separate sigmoidal lenses of brecciated carbonates. Sample URD13 belongs to one of these sigmoidal lenses.

3.3.1.3 Sub-unit c (Fig. 10A2)

Also against the fault but in the upper part of the exposure, orange-colored cataclastic dolostones of Late Triassic or Lower Jurassic age form meter-sized corrugations (sample URD18 and URD20). The strongly deformed dolostones develop towards the south and form symmetrical tectonic lenses separated by thin anastomozing shear zones. Here also, striations dip at high angle, but the shear sense criteria along the lenses are not clear. However, the geometry of the lenses indicates an overall flattening of the metasedimentary sequence perpendicular to the S0 plane. This deformation is consistent with an extensional regime during the main deformational event and a normal sense of shear along the main fault, in accordance with the fault-kinematic deduced from the geometry of the subunit-b tension gashes. A similar fabric is systematically observed in the Mesozoic sediments overlying the crustal mylonites of hill 488 and in the unit of Middle Jurassic limestones overlying the basement units of Soum d'Unars, thus suggesting an overall exhumation-related flattening of the pre-rift cover around the Urdach body (Fig. S2A, C, D, Supplementary Material). Very thin layers of a black material occur at some contact zones between the dolomites and the calcite-chlorite veins. They probably represent extremely sheared levels of organic matter and carbonates belonging to the next subunit. Locally oxidized iron-rich zones give the outcrops a pronounced orange color.

3.3.1.4 Sub-unit d (Fig. 10A2)

The dolomitic lenses of sub-unit c are in contact with sigmoidal lenses of black marbles cross-cut by abundant white calcite veins and by shear zones of black, laminated, phyllite-rich material (sample URD14). In the center of the exposure, a complex high strain zone is observed with lenses of orange dolostones alternating with lenses of black marbles.

3.3.1.5 Sub-unit e (Fig. 10A2)

After a zone of poor exposure, hard rocks composed of calcite, quartz and light-green micas (Cr-muscovite, see composition in section 2 of Supplementary Material) invaded by pyrite crystals are observed. Sample URD15 (Fig. 10D) was collected from a vertical, meter-wide metasomatic layer composed of anastomosing white carbonate veins including lenses of schistozed black rocks. These rocks display evidence of high strain with abundant and complex crosscutting relationships between quartz-calcite veins. They are tectonically associated with dolostone breccias also showing abundant veining (sample URD19). Both URD15 and URD19 samples record complex and imbricate fluid-rock interactions.

The studied section ends where vertical strata of the Upper Cretaceous flysch are observed, after a 20–30 m long zone lacking exposures.

3.3.2 The Peillou section

Complementary observations relative to the cover *décollement* close to the Urdach mantle body can be made to the north of the studied area, in the locality of Peillou (Fig. 4). Here, an association of strongly sheared Triassic and metasomatic rocks separated by vertical fault zones is exposed along the river. This site corresponds to a structural key-point where the continuations of both the Urdach crust-mantle detachment and cover *décollement* traces merge. In addition, the northern prolongation of the basal thrust of the Mail Arrouy anticline coincides with the site of the Peillou section. The most representative rock-types of the Peillou section are as follows, from NE to SW along the east side of the river:

- Grey brecciated calc-schists and talc-chlorite carbonated schists that display evidence of important metasomatic crystallizations. This tectonic breccia incorporates clasts of ultramafic composition as well as clasts of a more mafic protolith (chlorite-talc-rich sample BCOR300b);
- an albitite-like white granular rock, reminiscent of the albitic dikes that cross-cut the Urdach mantle (Pin *et al.*, 2001, 2006) (sample BCOR300a);
- a tectonic breccia including clasts of various origin in a grey to whitish granular microbreccia matrix. Most of the clasts apparently derive from Triassic protoliths, such as brecciated orange dolostones and rare meta-ophites (sample BCOR300c);
- a white granular rock spotted with numerous black crystals (possibly dark dolomite) (sample BCOR300e). This rock was found to be an anhydrite-bearing meta-evaporite from microprobe determination (see section 2 of Supplementary Material).

Unfortunately, the primary relationships between these various rocks cannot be clarified. The occurrence of Triassic and mantle remnants close to possible albitites, the latter being usually found intruding mantle rocks, would suggest that the Peillou association represents the northern trace of the Urdach cover *décollement*. Following this interpretation, the verticalized succession observed along the Peillou section can be considered as the result of tectonic inversion of a former extensional detachment. The location of the Peillou section in the northern prolongation of the Col d'Urdach exhumation complex also favors this interpretation.

3.3.3 Microscopic study and mineralogy: evidence for metasomatic transformations

This section appears in the text file of Supplementary Material.

4 First evidence of a post-exhumation volcanic event

We discovered a meter-thick layer of volcaniclastic rocks interbedded within the first levels of the Late Albian flysch. These rocks are exposed along the road cut, 10 m north of the contact between the Urdach lherzolite body and the flysch, close to the Bilatre quarry. The volcaniclastics are partly altered into a brownish rock composed of aggregated rounded clasts with brown to orange rims. Their less altered parts are composed of a grey to bluish spherulitic hard rock showing light grey, millimeter-thick chilled margins contrasting with the soft, brownish altered flysch layers. Centimeter-sized fragments of contorted light-brown flysch are included within the blue volcanogenic rock (Fig. S10, Supplementary Material). We sampled the altered and non-altered portions of the volcanic rocks as well as the chilled margins (BCOR274 and BCOR394). In thin section, the volcanic rock exhibits a typical spherulitic texture. Most of the spherulites are composed of microlitic volcanic material (Fig. S1, Supplementary Material). A minor portion consists of variably altered glass with flattened vesicles. In some thin sections, the ovalized spherulites are imbricated and/or welded, and display evidence for ductile deformation. Their alignment defines a rough foliation at the microscopic a rough foliation at the microscopic scale possibly due to syn-emplacement flattening. The lava spherulites are associated with two remarkable mineralogical components:

- isolated euhedral quartz crystals with numerous fluid inclusions;
- quartz-dominated polycrystalline fragments, some of them with an internal foliation and others showing ondulose extinction.

The first type resembles the evaporitic quartz, well known in the Keuper sediments, thus suggesting the presence of debris from a Triassic source. The second type most probably derives from a Paleozoic basement. Both types likely record the contact between the erupting magma and a continental basement unit before emplacement of the former over the ultramafic basement.

The major and trace element analysis of handpicked lava spherulites from a chilled margin (sample BCOR394d) is shown in Table 1, Supplementary Material. Despite their altered character (loss on ignition: 10.7 wt%) and their corresponding depletion in "mobile" alkali and alkali-earth elements, they have preserved a relatively intact "immobile" trace element signature typical of near-primary basaltic magmas (rather high MgO, Cr, Co and Ni contents). They

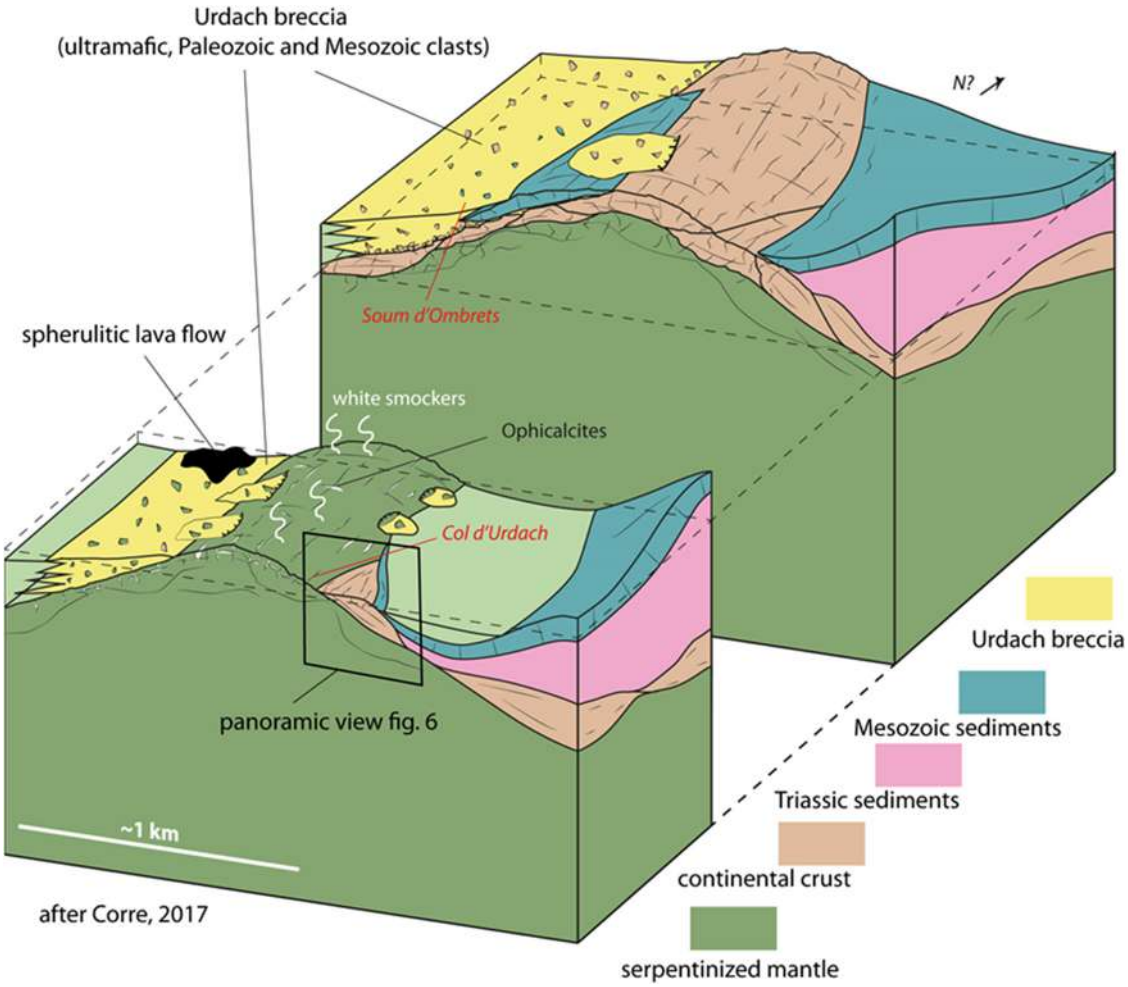

Fig. 11. 3D reconstruction of the floor of the Cretaceous NPZ basins in the exhumed mantle domain of the North Iberia margin, from the geology of the Urdach area (redrawn after Corre, 2017).
Fig. 11. *Reconstruction en 3D du plancher d'un bassin crétacé de la ZNP d'après la géologie du site d'Urdach (modifié d'après Corre, 2017).*

are rich in high field strength elements (Nb, Zr, Ti), in rare earth elements (REE) and in Th. Their normalized multielement pattern (not shown) is highly fractionated, with concentrations in the most incompatible elements (Th, Nb, La) reaching c. 200 times the Primitive Mantle values. Such uncommon enrichments are typical of nephelinites and related strongly silica-undersaturated lavas from intraplate and rift settings, that are thought to derive from very low melting degrees of enriched mantle (Wilson, 1989; Wilson and Downes, 1992).

5 LA-ICP-MS U-Pb dating of zircons

This section appears in the text file of Supplementary Material.

6 Discussion

Based on the geological and geochemical data reported above, we now discuss issues relative to the evolution of the northern Iberia margin along the following six subsections: a 3D reconstruction of the distal domain (section A), the deformation of the exhumed mantle (section B), the fluid-rock interactions in the extensional detachments (section C), the significance of serpentinization and mantle carbonation of the Urdach mantle with respect to current oceanic references (section D) and the significance of the volcanic event discovered in the very first levels of the post-exhumation Late Albian flysch (section E). We finally discuss the significance of the ages obtained on in situ zircons (section F).

6.1 3D architecture of the distal domain of the Iberia margin

We first list the main constraints that are necessary to our 3D reconstruction:

– new mapping of the Urdach massif reveals that Paleozoic crustal mylonites form small lenses still welded on the exhumed mantle. The internal foliation of the lenses remarkably parallels the contact with the mantle rocks and the alignment of the tectonic lenses of the lenticular layer (see Asti *et al.*, 2019, for more details). Therefore, a critical

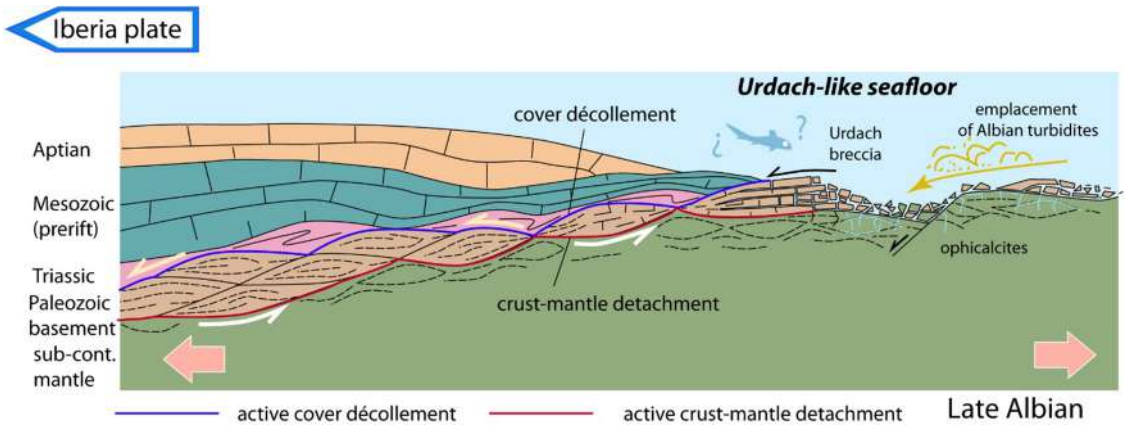

Fig. 12. Cartoon to describe our interpretation of the crust-mantle detachement (red) and cover *décollement* (blue) interactions in the mantle exhumed domain. This figure depicts our interpretation of the genesis of the Urdach breccia by exhumation of tectonic breccia followed by gravity-driven reworking on the seafloor. Note the strong boudinage and tectonic attenuation of the pre-rift cover and the disruption of the Triassic layer in relation with high-displacement along the cover *décollement*.

Fig. 12. *Les interactions entre le détachement croûte-manteau et le décollement de couverture dans la marge distale nord-ibérique.*

feature from the Urdach massif is the parallel attitude of both mantle and crustal rocks fabrics indicating that they were deformed contemporaneously during a large part of the mantle exhumation process. Moreover, radiometric dating of the mylonitization in the continental crustal unit at hill 488 confirms the Late Albian age of this deformation and its direct link with the processes of mantle exhumation (Asti *et al.*, 2019);

– from detailed petrological investigation of the Variscan material, Asti *et al.* (2019) argue that during mantle exhumation along the crust-mantle detachment, the overlying continental crust first was deformed in the ductile regime, (at ca. 450–350 °C), then crossed the ductile/brittle transition (cataclastic breccias) before exposure to the seafloor together with the shallowest layers of the exhumed mantle. As a result, both the fractured serpentinized lherzolites and the brecciated continental mylonites were involved in sedimentary processes resulting in the accumulation of the Urdach breccias during the Late Albian (Debroas *et al.*, 2010; Lagabrielle *et al.*, 2010; Canérot, 2017a, 2017b). The cataclastic crustal breccias precursor of the Urdach breccia are exposed in a few places (Soum d'Unars, Mer de Her) where they are found locally silicified. They likely formed close to the merging point between the crust-mantle detachment and the cover *décollement* (Figs. 11 and 12). In addition, the lithological content of the Urdach breccia indicates that the Paleozoic lenses outcropping on the floor of the Albian basins are devoid of lower and uppermost crustal levels and were extracted mostly from mid-crustal levels (Ordovician quartzites, Silurian schists, and granitoid) (Asti *et al.*, 2019). This provides a key-constraint to the reconstruction of the tectonic evolution of the continental crust during the margin evolution;

– the cover *décollement* corresponds to the surface along which the Triassic succession underwent metasomatic transformations and was by place intensively tectonized. Moreover, the Triassic material is locally entirely removed by basal truncation. This is well observed in the Urdach "ball trap" section where Liassic rocks are found in direct contact with the mantle rocks. In addition, the entire Mesozoic sequence thins drastically approaching this contact, in relation with the detachment evolution. This is well-observed on the geological map (Casteras *et al.*, 1970 and Fig. 4). By contrast, Keuper sediments are preserved in the Peillou section as lenses talc-chlorite schists, cataclastic dolostones and polymictic breccias with anhydrite clasts. These results lead to a reconstruction of the Cretaceous distal margin with a boudinaged Triassic layer composed of an assemblage of cataclastic breccias and metasomatic schists. Similar features arise from the study of the Saraillé massif (see companion paper, Lagabrielle *et al.*, 2019).

Based on these geological constraints, we propose a 3D reconstruction of the distal domain of the Iberia margin. Figure 11 is a block-diagram resulting from the retro-deformation of the Urdach fold (Corre, 2017). It shows a composite basement in the final stages of the exhumation, when displacements along the crust-mantle detachment ceased. The reconstructed landscape, with a rough morphology, is made up of areas exposing either serpentinized mantle or brecciated crustal mylonites in response to the intense thinning that occurred during lower units exhumation (Fig. 12). Ophicalcites develop in the shallow level of the ultramafic basement with hydrothermal fluids expelled from white smokers widespread on the seafloor, as currently observed at some Mid-Atlantic Ridge sites (e.g. Lost City hydrothermal field, Denny *et al.*, 2015). Disaggregation of the cataclastic breccias provides the material reworked in the sedimentary breccias accumulating in screes and debris-flows deposited at the base of the scarps (Urdach breccia). Some reliefs are formed by remnants of the pre-rift sedimentary cover that are abandoned when motion along the cover-*décollement* ceased. The deposition of the Late Albian flysch starts on this composite seafloor. Volcanic activity occurs locally, during the emplacement of the first turbidites.

6.2 Deformation of the exhumed mantle

In the Urdach massif, the mantle rocks situated beneath the paleo-seafloor are characterized by a lenticular fabric very similar to that described in the Saraillé massif (see companion paper Lagabrielle *et al.*, 2019). The lenticular fabric is observed at least in the first 100 m of the uppermost mantle around Col d'Urdach and along the western side of the Urdach body. Most of the large ultramafic blocks reworked at the base of the Urdach breccia close to the Bilatre quarry also display anastomosing metric shear zones typical of the fabric in the lenticular layer (Fig. 7I). We thus deduce that at the final stages of the mantle exhumation process, the tectonic lenses of the Urdach lenticular layer were exposed to the seafloor and provided pre-fractured material reworked in the neighboring clastic sedimentation.

Displacement at the crust-mantle interface during the exhumation is not concentrated along a single fault surface but is distributed in the first levels of the exhumed mantle. It is achieved through motions along the multiple gliding planes bounding the tectonic lenses of the lenticular layer (Fig. 12). Hydration responsible for synkinematic growth of serpentine in veins concentrates in this tectonically active part of the mantle and induces mechanical weakening as demonstrated by numerous studies of ultramafic oceanic environments (Karson *et al.*, 2006; Boschi *et al.*, 2006a, 2006b; Picazo *et al.*, 2012).

Three well-studied oceanic sites exhibiting present-day active exhumation of mantle rocks along the slow-spreading Mid-Atlantic Ridge, known as oceanic core complexes (OCC), bear similarities with the Urdach lenticular deformation:

- in the Atlantis OCC, the distribution of brittle deformation with depth suggests that low-temperature strain is concentrated along a series of low angle faults within several hundred of meters of the domal surface (Blackman *et al.*, 2002). The upper detachment is about 100 m thick and is characterized by strongly foliated to mylonitic serpentinites and talc-amphibole schists (Karson *et al.*, 2006). A few faults, rather than a single detachment, accommodate the uplift and evolution of this oceanic core complex, and the deformation is widespread along sigmoidal lenses at the kilometer scale. Studies of rocks drilled and dredged within a few tens of meters below the exposed corrugated surfaces of this OCC indicate significant strain weakening associated with the synkinematic growth of weak hydrous minerals such as serpentine, amphibole, chlorite and talc (Escartin *et al.*, 1997, 2003, 2008; Schroeder *et al.*, 2002; Boschi *et al.*, 2006a, 2006b);
- disruption of oceanic basement rocks along anastomosing shear bands in extensional detachments is also well observed along the OCCs south of the 15°20 FZ (Escartín *et al.*, 2017). There, the detachment fault zone includes a set of anastomosing slip planes defining spectacular lenticular fabrics at a meter scale. In addition, the deformed material provides abundant screes that accumulate in aprons showing affinities with the Urdach breccia;
- on the OCC at N 15°48′, samples from the striated surfaces are dominated by fault rocks with low-angle shear planes and highly deformed greenschist facies assemblages that include talc, chlorite, tremolite, and serpentine. Deformation is very localized and occurred in the brittle regime. Penetration of fluids along preferential permeable pathways induced marked weakening with crystallization of serpentine and secondary minerals (e.g., talc, chlorite), localizing strain very efficiently into large, discrete shear zones within the shallow lithosphere (MacLeod *et al.*, 2002).

This comparison with oceanic situations stresses that similar deformation modes involving disruption of hydrated mantle into tectonic lenses along low-angle extensional faults at all scales, are found in both ridge environments and paleo-passive margin exhumation domain. This confirms similarities in mantle exhumation processes between margin and ridges established and discussed by previous authors (Cannat *et al.*, 2009).

Most of the meso-scale structures observed in the lenticular layer point to a symmetrical pattern indicating generalized flattening (possibly multidirectional) rather than monodirectional shearing. Flattening (which occurred in the serpentinization field) might thus be linked to the last deformation events, in relation with doming of the unroofed mantle. Due to the poor conditions of exposure, we could not obtain more microstructural data from the lenticular layer than those exposed in Figure 4 and we certainly missed important information relative to the deformation mode along the main fault zone at the top of the lenticular layer.

Considerable displacement at the crust/mantle interface is required during mantle exhumation and unroofing. This displacement cannot be accommodated by flattening and localized simple shear necessarily occurred along restricted main faults forming the crust-mantle detachment. Pervasive flattening may have been dominant in the center of the basin once the mantle was close to the surface. Symmetrical boudinage and conjugate shear bands related to overall flattening are indeed well observed in the first levels of the Cretaceous flyschs deposited over the thinned pre-rift cover (Corre *et al.*, 2016, 2018). Therefore, we may infer that simple shear was dominant along the detachments in the first rifting stages, whereas pure shear dominated the syn- to post-rift evolution before the onset of compression in the Santonian (Fig. 3).

6.3 Fluid-rock interactions in the extensional detachments

Based on the studied mineralogical assemblages, a variety of fluids were involved in producing the metasomatic rocks that crystallized within the footwall and hanging wall of the Urdach crust-mantle detachment and cover *décollement*. In the following, we discuss our main results regarding metasomatic processes along these fault zones (Fig. 13).

6.3.1 Serpentinization and carbonation

The lenticular layer of the deformed mantle at Col d'Urdach displays two types of serpentine. In the massive mantle, the pseudomorphic serpentine replaces former peridotite minerals in situ, whereas serpentine in veins crystallized out of the peridotite, from a Mg-Si-bearing metasomatic fluid derived from the mantle rocks alteration as described by Andreani *et al.* (2007) in oceanic environments.

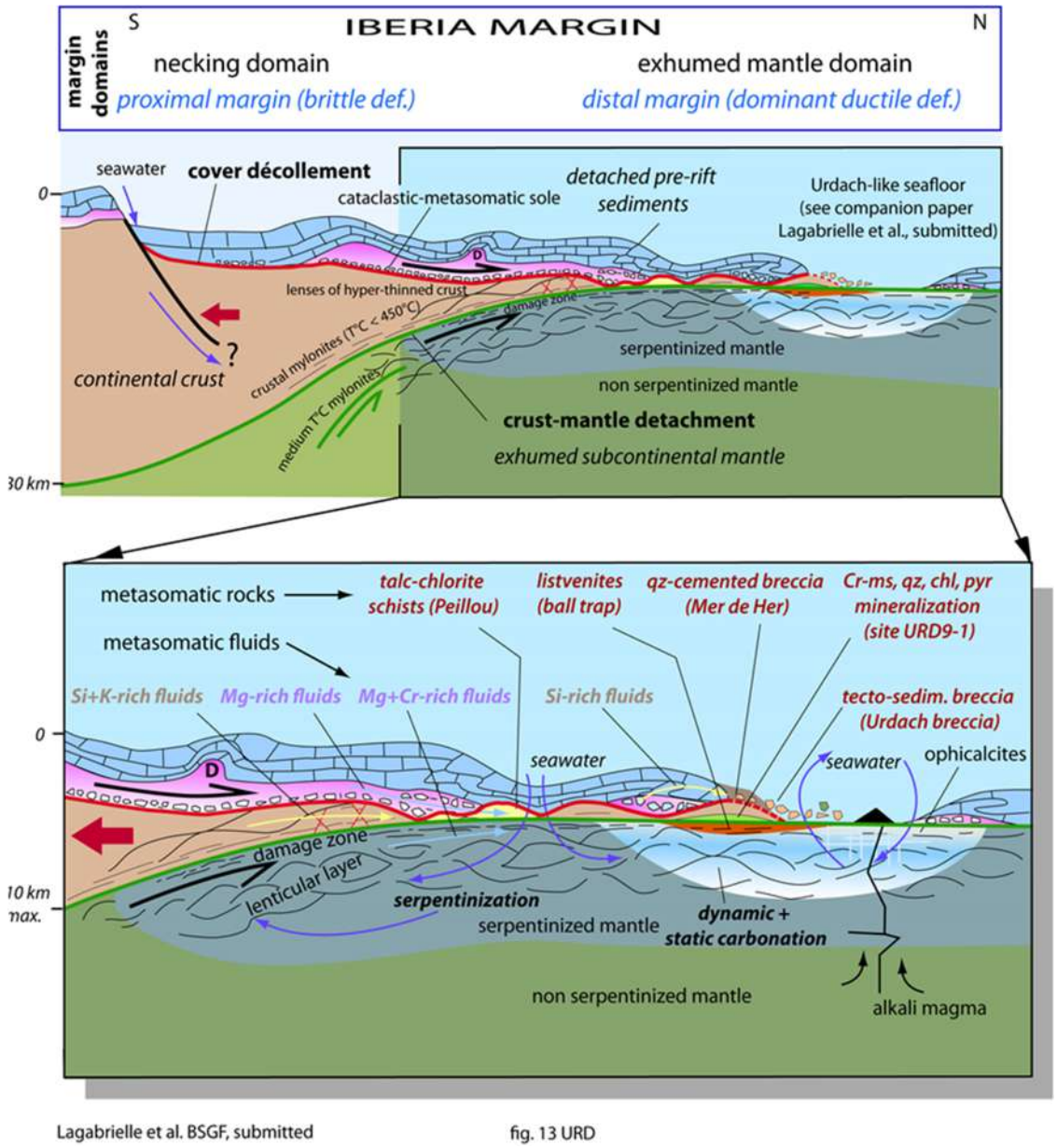

Fig. 13. Architecture of the North Iberia distal margin and fluid-rock interactions in the exhumed mantle domain based on this study. Complementary information based on the study of the nearby Saraillé massif can be found in the companion paper Lagabrielle et al. (2019).
Fig. 13. *Architecture de la marge nord-ibérique et schéma de la circulation des fluides associée au fonctionnement des grands détachements.*

Our preliminary chemical study points to a difference in compositions between both types. Serpentine in veins are relatively Al- and Fe-poor (sample URD17a, Table 10 in Supplementary Material) suggesting that serpentine-rich fluids do not preferentially export these elements from the mantle. In the "ball trap" section (Fig. 10), the serpentine in veins belong to metasomatic fault-rocks and alternate with elongated calcite-rich lenses (sub-unit b) indicating that serpentinization occurred synchronously with the carbonation while the cover *décollement* was active. Therefore, the fault rocks of sub-unit b can be considered as syntectonic ophicalcites.

Insights from our study of the samples of the Bilatre quarry is that carbonation of the Urdach mantle is restricted to the upper levels of the lenticular layer and exhibits evidence of multi-phased alteration process with a first diffuse in-situ carbonation followed by carbonation in veins. The early pervasive carbonation was followed by a fracturing stage during which the carbonated lherzolites expanded. Precipitation of vein calcite started at the sheared edges of the tectonic lenses in the lenticular layer. Then orthogonal veins were filled by successive generations of calcite precipitates cutting across the previous syn-kinematic veins, as demonstrated by textural analyses of samples URD1 and URD12 (Figs. S4 and S5, in Supplementary Material). Volume increase of the host rocks requires lowering of the lithostatic pressure that can be achieved only when the serpentinized mantle reaches the

Earth's surface. Syntectonic carbonation is also argued from the examination of the lenticular layer in the Saraillé mantle body (see companion paper Lagabrielle *et al.*, 2019).

These features collectively support the interpretation of the Urdach cover *décollement* as a preferential pathway for serpentinization and carbonation-related fluids during mantle exhumation. Mantle-derived fluids expelled from active serpentinization regions circulated along the crust-mantle detachment and the cover-*décollement* and triggered the co-crystallization of serpentine and calcite. Fluid circulation is favoured by the porosity linked to brittle failure along the crust-mantle detachment. Therefore, we stress that calcite veins forming the ophicalcite network of the Bilatre and Col d'Urdach quarries represent fossilized plumbing of the hydrothermal system and define paleo-fluid flow-paths that developed on the ultramafic seafloor of the NPZ Albian basins. Similar systems are reported from well-studied current serpentine-hosted hydrothermal sites (Ludwig *et al.*, 2006).

6.3.2 Cr-rich fluids and listvenites in the cover *décollement*

Besides serpentine in veins, the influence of mantle-derived fluids is well expressed in the "ball-trap" and Peillou sections by the prevalence of metasomatic minerals enriched in elements that are abundant in mantle rocks. The presence of Cr in the structural formulae of chlorites from fault rocks and the occurrence of listvenites are the most obvious expression of the influence of fluids that leached peridotites. Such presence of Cr in chlorites and micas indicates that this element circulated as a solution after being extracted from the lherzolite by fluids able to partially dissolve the spinel.

According to Plissart *et al.* (2009), the formation of listvenite is a three-fold metasomatic process in a serpentine-rich protolith that involves:

- carbonation;
- silicification;
- Cr-rich mica formation.

The related Si and K additions contained in quartz and fuchsite respectively, require external sources, which would imply either a leaching of crustal felsic units or a direct input from felsic intrusions. Input of Si may also be produced internally through the serpentinization process. A contribution of sea-water derived fluids can be envisioned for the K enrichment (Plissart *et al.*, 2009). Another mechanism to enrich listvenites in Si is the Mg-depletion of the peridotite, as shown by mass-balance calculations in serpentinized peridotite clasts from Devonian formations of Norway (Beinlich *et al.*, 2010). Listvenite-rich transformations are reported from numerous extensional as well as compressive settings. P-T conditions for the formation of all listvenites worldwide correspond to the greenschist facies ($200\,°C < T < 400\,°C$, $1 < P < 3$kbar) (Halls and Zhao, 1995; Harlov and Austrheim, 2013). Therefore, the conditions for the formation of the Urdach listvenites are consistent with a Raman Spectroscopy of Carbonaceous Material (RSCM) temperature of 300 °C obtained for sample URD14 collected in the Urdach cover *décollement*, close to the sample URD15 listvenite.

In oceanic environments, listvenite formation characterizes a medium-temperature (~300 °C) metasomatic stage overprinting a previously warmer (> 450 °C) ocean-floor metamorphism (Plissart *et al.*, 2009). Listvenite formation may also occur by:

- hydrothermal alteration of the lithospheric mantle caused by slab-derived fluids circulation during subduction at active continental margins (Menzel *et al.*, 2018);
- during the obduction of ophiolitic sheets;
- during orogenic processes under the influence of fluids deriving from overthrusted sialic units (Rodriguez Garcia *et al.*, 2015; Beinlich *et al.*, 2012).

Finally, like in these three tectonic settings, the involvement of a sialic crust may account for the Urdach listvenite Si and K budgets. The mylonitic gneisses from the nearby hill 488 or the metasomatized suite from site URD9-1 for example, are valuable candidates to provide the Si and K elements needed.

6.3.3 Mantle- and continent-derived fluids in the crust-mantle detachment

The crust-mantle detachment at site of sample URD9-1 is associated with a group of metasomatic rocks composed of euhedral chlorite flakes in a groundmass of white feldspars cross-cut by a series of chlorite-quartz rich veins and listvenite-like rocks including pyrite mineralization in their core. This complex rock suite appears to be entirely metasomatic and crystallized in the crust-mantle detachment at the base of the tectonic lenses of Paleozoic material that form the relief of Soum d'Unars. The metasomatic fluids that promoted this assemblage circulated in successive episodes as evidenced by the tectonic fabric at the thin-section scale. These fluids exchanged elements that may be of local derivation such as Cr and Mg (mantle rocks), Na (albitites) and Si (continental crust). They have affinities with the fluids involved in the formation of the "ball trap" listvenites suggesting some connection between the plumbing systems of the crust-mantle detachment and cover *décollement*.

6.3.4 Sulfidation

Most of the rocks associated to both the Urdach crust-mantle detachment and cover *décollement* fault zones contain abundant pyrite in association with other newly-formed minerals and this widespread sulfidation is also strong evidence for metasomatism. In a dual continental/oceanic tectonic context, the most probable source of S^{2-} may be the TSF (thermo-sulfate reduction), a process that is initiated at temperatures as low as ca 100 °C by reacting a SO_4^{2-}–bearing fluid (sea-water or fluid leaching Triassic evaporites) with organic matter (Machel, 2001). This process has been documented for gas resource in the Lacq field (Aquitaine basin) and has been compared to processes that occurred close to the Saraillé mantle body (Corre *et al.*, 2018). It is highly plausible in the Chaînons Béarnais because many rocks of the pre-rift sedimentary pile contain abundant organic matter (e.g. sample URD14, see also Biteau *et al.*, 2006). Field evidence both in the Urdach and the Saraillé sites show that once produced, the fluids carrying sulfide ions were trapped and circulated preferentially along the crust-mantle detachment and cover *décollement* fault zones.

6.3.5 Triassic-derived fluids

As a result of tectonic elision during the exhumation process, both the cover *décollement* and the crust-mantle detachment of the Urdach massif are devoid of Triassic formations, with the exception of the Peillou section where meta-evaporites and associated cataclastic rocks remain. However, it is noteworthy that even in the places where the Triassic rocks are lacking, the presence of fluids of Triassic derivation is still recorded along the detachment faults. In their study of the basal Urdach breccia at Mer de Her, Nteme (2017) demonstrate the influence of fluids expelled from the deforming Triassic sole, now disappeared. Their petrographic, microthermometric and Raman spectroscopy analyses of bi- and tri-phases fluid inclusions in quartz cements show that high-salinity fluids circulated at the base of the detached pre-rift cover and allowed the precipitation of quartz in the Mer de Her tectonic breccias emplaced in the crust-mantle detachment. Corre *et al.* (2016) also evidenced the influence of Triassic brines in fluid inclusions inside veins cross-cutting the Jurassic and Cretaceous carbonates of the Saraillé pre-rift sequence above the Saraillé cover *décollement*.

In the Peillou section, remnants of Triassic lithologies such as meta-evaporites are the witness of the presence of a more complete Triassic sequence before the mantle exhumation process initiates. Moreover, the occurrence of metasomatic rocks and cataclastic breccias involving Triassic material (ophites, dolomites) highlights the deep transformation that occurred in the sole of the detached pre-rift cover during displacement along the cover-*décollement*. The well-known lubricating tectonic behaviour of the Triassic material (e.g. Soto *et al.*, 2017) is a major characteristic of the pre-rift cover at a regional scale and accounts for key-characteristics of the Chaînons Béarnais structure and more generally of the whole NPZ (Clerc and Lagabrielle, 2014).

6.4 Urdach mantle serpentinization and carbonation: a comparison with metasomatic processes at slow-spreading active oceanic ridges

Studies of detachment surfaces along slow-spreading mid-ocean ridges show that serpentinization activates hydrothermal cells involving zones of fluid input and zones of discharge separated by pluri-kilometric distances (Mével, 2003; Karson et al., 2006; Boschi *et al.*, 2006a; Pinto *et al.*, 2015). At slow-spreading ridges and in alpine-type ophiolites, mantle carbonation is linked to active serpentinization. In these settings, CO_2-rich fluids produced by the serpentinization of large volumes of peridotites trigger the total dissolution of the serpentinized silicates and their replacement by carbonates, most often calcite (e.g. Kelemen *et al.*, 2011; Lafay *et al.*, 2017 with references therein). Geochemical studies of vein calcites in active hydrothermal sites show that serpentinization produces highly reducing conditions and results in the partial reduction of seawater carbonate to methane at temperatures of 250 °C (Alt and Shanks, 2003).

In the following, we propose a short report of data from four emblematic sites, enlightening possible conditions that prevailed during the Urdach detachment-faulting period.

In the serpentinized mantle of the Kane FZ (central MAR, 23 °N), the first episode of serpentinization is interpreted as the early tectonically controlled penetration of seawater-dominated fluid within peridotites, enhancing thermal cracking and mesh texture initiation at 3–4 km up to 8 km depth and at T < 300–350 °C (Delacour *et al.*, 2008a). Following Alt and Shanks (2003), the sulfide oxide mineral assemblage, high sulfur contents, and silicate mineral stabilities indicate that the main stages of serpentinization took place at 300 °C.

In the Lost City hydrothermal field at the Atlantis FZ OCC, serpentinization and talc-metasomatism are a direct result of mantle denudation. As reported earlier, active serpentinization is responsible for producing highly reducing environment characterized by high-pH fluids containing abundant dissolved hydrogen and methane. The rates of serpentinization are likely to be highest at temperatures of ~250 °C. Hydration and diffusion rates are notably low below 100 °C (Früh-Green *et al.*, 2003). Hydrothermal outflows of fluids at temperature of 40–90 °C produced by the active serpentinization of the unroofed mantle, construct chimneys up to 60 m-high of carbonate and brucite. These hydrothermal sites are located at the intersection between widely spaced, steeply dipping normal faults and the dome-shaped, early detachment zone. Isotopic studies of veins and bulk carbonates in the mantle basement indicate precipitation temperatures in the range of 225 °C to 50 °C (Früh-Green *et al.*, 2003; Delacour *et al.*, 2008b).

In the hydrothermally altered peridotites drilled in the 15°20′ N Fracture Zone area on the Mid-Atlantic Ridge, the breakdown of olivine to serpentine, magnetite, and brucite occurs at temperatures below 250 °C (Bach *et al.*, 2004, ODP Leg 209). In the Galicia-Iberia exhumed mantle, the main serpentinization event occurred at a temperature below 300 °C, and possibly down to 50 °C, as a consequence of the introduction of a large amount of seawater (Agrinier *et al.*, 1988). Later on, calcite derived from seawater impregnated pervasively the peridotite and precipitated locally in fractures at low temperature (10 °C).

In the Chenaillet massif, isotope analyses of different generations of carbonates in cross-cutting veins support a relatively high temperature for carbonate formation, i.e. up to 170 °C for the carbonate matrix co-precipitating with serpentine. Late calcite veins are characterized by a lower temperature of 120 to 150 °C (Lafay *et al.*, 2017).

This comparative dataset leads us to propose a thermal scenario applying to serpentinization and carbonation of the Pyrenean mantle bodies. Serpentinization is shown to be efficient in the range of 450–300 °C, with rare cases of lower temperature serpentinization (Galicia margin), while carbonation may occur between 150 and 20 °C. Therefore, serpentinization and coeval deformation in the lenticular layer of the Urdach peridotites may have started when the mantle was still at a depth of several km, in high-grade greenschist facies conditions. By contrast, carbonation most likely occurred under lower temperature conditions when the mantle was closer to the surface. The final carbonation stages occurred when the mantle rocks were able to expand in brittle conditions, that is very close to the seafloor.

6.5 Mantle exhumation and magma production

The nephelinite-related volcanic rocks interbedded within the first levels of the Late Albian flysch near the Bilatre quarry

(Figs. S10 and S11, Supplementary Material) are the first record of volcanic activity that emplaced its materials almost over exhumed mantle rocks along the NPZ. Their very high La/Yb ratios and high Yb contents (Table S1) are consistent with their derivation from c. 1% melting of an enriched spinel-rich lherzolitic mantle according to the models developed by Luhr *et al.* (1995). The spherulitic texture of the studied samples is likely related to an explosive emplacement with water interaction. Similar interactions with pillow-lavas, hyaloclastites and volcaniclastic breccias are described in volcanic successions of same age from the Basco-Cantabric basin (Castanares *et al.*, 1997, 2001). Very close to Urdach, in the Oloron area, subaqueous basaltic lava flows and many intrusive bodies are also exposed (Casteras *et al.*, 1970). Intrusions consist of alkali dolerite sills (up to several tens of metres thick), locally fractionated into picrites, teschenites and analcime syenites (Azambre and Rossy, 1976; Azambre *et al.*, 1992). Timing of emplacement of magmatic rocks is constrained by K-Ar dating between 113 and 85 Ma (e.g. Montigny *et al.*, 1986). Interbedded sediments have been dated with microfossils at the Albian-Cenomanian boundary in the Oloron area (Schoeffler *et al.*, 1964). In the Basco-Cantabric basin, the Errigoiti Formation is the largest of several volcanic complexes of Albian to Santonian age widespread between Gernika and Plentzia (Castanares *et al.*, 1997). It consists of a bathyal alkali submarine volcanic system that includes sheeted lavas, pillow lavas, pillow breccias and stratified breccias deriving from volcaniclastic resedimentation through gravity flows (Castanares *et al.*, 2001).

In the Chaînons Béarnais, alkali dikes and sills are mostly emplaced in the Cretaceous flysch formations and are rarely found cutting through Mesozoic sediments and Paleozoic lenses. This suggests that alkali magmas erupted preferentially in the exhumed mantle domain, in regions devoid of crustal cover and forming windows opened over exhumed serpentinized peridotites. Due to its stratigraphic position, the Urdach volcanic episode occurred during the Late Albian. Thus, it was nearly coeval with the emplacement of the corundum-free and corundum-bearing albitite dikes in the Urdach and Espechere bodies dated at 101 ± 2 Ma by Pin *et al.* (2001). The albitite dikes are interpreted as very-low-degree partial melts produced at relatively shallow depth in enriched subcontinental peridotites, in a rapidly uplifting mantle block, as a result of the strong thinning of the lithosphere beneath the North Pyrenean rift during mid-Cretaceous times (Pin *et al.*, 2001, 2006). Pressure of generation of the Pyrenean felsic melts ranges from 0.5 to 0.7 GPa (Pin *et al.*, 2001), in broad agreement with the latest stage of equilibration (0.6 to 0.7 Gpa i.e. 20–30 km depth) recorded in lherzolites from the region (Fabriès *et al.*, 1998). Therefore, a genetic link between the parental magmas of the Urdach nephelinites and the albitite dikes can be envisioned, as they both derived from very low melting degrees of a spinel lherzolite source.

Finally, the discovery of lavas in Cretaceous flysch at Urdach is not surprizing since the NPZ and the Basco-Cantabric basin are characterized by the emplacement of alkali magmatic products during the Albian-Santonian times. All the geological data collected both in the Urdach mantle rocks and in their sedimentary-volcanic cover argue for a very rapid uplift, caused by tectonic denudation bringing mantle peridotites to unusually shallow depths. Following Pin *et al.* (2006), this uplift was instrumental in the generation, segregation, and tapping of enriched, very low degree partial melts.

6.6 Significance of zircon ages obtained in this study

Poor conditions of exposure preclude any detailed analysis of the field relationships between the mantle rocks and the sericitized feldspar- and albite-rich rock that displayed the Concordia date of 112.9 ± 1.6 Ma (sample URD9-1). However, based on mineralogical composition affinities, we may infer that the URD9-1 sample represents an albitite dike similar to previously described albitite dikes intruding the mantle rocks at 101 Ma (Pin *et al.*, 2001, 2006). Our zircon age is slightly older than Pin *et al.* (2001) ages, which may indicate a time span of at least 10 Myr for the emplacement of the Urdach albitite dike swarm. This age, however, is consistent with the age of 105–108 Ma obtained on a gabbro dike from Urdach by Masini *et al.* (2014).

Chloritites are described as centimeter-wide zones at the boundaries of the corundum-bearing albitite dikes (Pin *et al.*, 2006; Monchoux *et al.*, 2006). They are also abundant at site of sample URD9-2 where they crystallized in metasomatic veins and shear bands in the crust-mantle detachment together with Cr-micas and amphiboles. Therefore, the zircon date (109.4 ± 1.2 Ma) obtained on sample BCOR115 from the Urdach breccia (sample origin remains uncertain) needs to be discussed. Static chloritization led to complete obliteration of the original texture in sample BCOR115 and it is thus difficult to precisely determine which was the original protolith of this metasomatized rock. However, zircon grains from this sample display several striking analogies with those of the magmatic albitites intruding the ultramafic Urdach massif (e.g. size, morphology, high Th/U ratio, crystallization age). These analogies allow to reasonably propose that the protolith of the chloritized sample BCOR115 was a magmatic albitite dike analogue to those intruding the Urdach mantle. Textural relationships suggest that intense static chloritization (growth of chlorite rosettes) postdate zircon crystallization, and likely represents the record of a hydrothermal event that altered albitite dikes after their emplacement at depth, in relation with circulation of metasomatic fluids during mantle exhumation. Whatever the case, the ages obtained here confirm that the various processes linked to the uplift of the subcontinental mantle beneath the opening basins of the future NPZ initiated during the Albian period. These processes range from mantle partial melting to metasomatic transformations through circulation of fluids from various origin (mantle- and continent-derived fluids). They are synchronous with metasomatic processes evidenced in the NPZ basement and in the Axial Zone as early shown by Schärer *et al.* (1999), Poujol *et al.* (2010) and recently completed by Fallourd *et al.* (2014).

7 Conclusions

1. The Urdach massif is composed of a remarkable association of serpentinized ultramafic and continental Paleozoic basement rocks. It bears the composite geological record of the processes leading to the extreme thinning of the distal part of a passive continental margin, ending with local

complete denudation of the subcontinental mantle. The parallel attitude of the mantle and crustal rocks fabrics in the Urdach massif indicates that both rocks were deformed coevally during a large part of the mantle exhumation process.

2. The mantle was exhumed towards shallow levels by displacement along the crust-mantle detachment, a ±100 m thick fault zone with a basal lenticular layer of serpentinized mantle lenses separated by anastomosing shear zones made up of sheared serpentinites. This fault zone acted as a pathway for the serpentinizing fluids (Fig. 13).

3. Serpentinized mantle rocks in the crust-mantle detachment exhibit evidence of local pervasive carbonation with primary silicates and serpentine replaced in situ by calcite. Calcite precipitation also occurred in veins, in the serpentine-rich shear zones separating the tectonic lenses of the lenticular layer and in a network of orthogonal veins when the mantle reached the seafloor (Bilatre and Col d'Urdach ophicalcites). These calcite veins are interpreted as the fossilised hydrothermal plumbing system and define paleo-fluid flow-paths that developed on the ultramafic seafloor of the NPZ Albian basins in response to tectonic and hydraulic stress.

4. The cover *décollement* is a thick fault zone corresponding to the tectonic sole of the pre-rift detached cover. This sole provides numerous evidence for metasomatic transformations with mineralogical assemblages formed in greenschist facies conditions that record the circulation of fluids from various origins, which precipitated Mg (serpentinization and chloritization), Si and K (listvenitization) (Fig. 13). These fluids circulated in the mantle, in the Paleozoic crust and in the Triassic sole at the base of the detached pre-rift cover. Multi-sources fluid-rock interactions and systematic greenschist facies conditions revealed by the metasomatic assemblages in the Urdach detachment faults imply that although they might have been reactivated during the Mail Arrouy thrusting, these faults cannot be newly-formed Pyrenean faults related to the contractional stages of the orogeny.

5. Greenschist facies conditions obtained for the studied fault zones are consistent with paleotemperatures deduced from clinochlore compositions in the Saraillé cover *décollement* (200–350 °C, Corre *et al.*, 2018), in agreement with previous estimates of 250–350 °C by Fortané *et al.*, (1986), Clerc *et al.* (2015) and Gaudichet (1974). Finally, during the mid-Cretaceous Pyrenean rifting, temperatures at the level of the crust-mantle detachment never exceeded 350 °C (Urdach, this study) or 450 °C (Urdach and Saraillé, Asti *et al.*, 2019). These temperatures cannot lead to the partial melting of the continental remnants associated with the lherzolites, even in the most distal part of the exhumation system. This result may be considered as a new thermal benchmark in further modelling of crustal thinning during the evolution of ductile-type passive margins (Clerc and Lagabrielle, 2014).

6. The dating of zircon grains contained in the albite-chlorite and chlorite rocks of the Urdach crust-mantle detachment confirms the Albian age of albitite dikes cross-cutting the peridotites (112.9 ± 1.6 Ma and possibly 109.4 ± 1.2 Ma), only some m.y. before the final exposure of the mantle to the seafloor, which is dated stratigraphically to the middle-late Albian (108–100 Ma) (Roux, 1983; Debroas *et al.*, 2010).

7. The spherulitic lavas with nephelinite affinity interbedded within the first levels of the Late Albian flysch near the Bilatre quarry record for the first time a volcanic event that emplaced its products over the mantle rocks, which at that time were almost exposed to the seafloor. Magmas were thus erupted preferentially in the exhumed mantle domain, in regions devoid of crustal cover. This event was nearly concomitant with the emplacement of the corundum-free and corundum-bearing albitite dikes dated at 101 ± 2 Ma (Pin *et al.*, 2001) in the Urdach mantle, and these two rock types can be considered as genetically linked (in a broad sense) since they both derive from very low melting degrees of an enriched spinel lherzolite source. This volcanic event also relates to the numerous alkali sills and dikes emplaced in the overlying Upper Cretaceous flysch sequence.

Finally, these data collectively allow us for the first time to propose a 3D-reconstruction of the distal margin domain of the North Iberia passive margin at the end of the Cretaceous extensional event. This reconstruction may help better constraining further interpretation of the strain pattern, P-T conditions, and fluid pathways in the distal portions of present-day passive margins where direct observations remain difficult. This study confirms that the Pyrenean belt represents a unique target for examinating pre-orogenic structures in mountain belts. Due to its short convergence rate (less than 100 km along the western transect), the Pyrenean belt exposes relatively well-preserved distal margin domain remnants. These remnants that form the remarkably continuous NPZ, are often buried at great depth under mountain belts showing larger convergence rates.

Supplementary Material

TEXT FILE (content : 1. text of sections 3.2.4, 3.3.3 and 5; 2. Detailed captions of figures S1 to S11 and tables S12 to S20).
Fig. S1. Field aspects of the Urdach breccia and views from the Mer de Her area.
Fig. S2. Deformation and fluid-rock interactions in the Mesozoic cover above the Urdach cover décollement.
Fig. S3. Microscopic view of the serpentinized Urdach mantle (sample URD4).
Fig. S4. The Bilatre quarry ophicalcites: sample URD1, hand specimen and microscopic aspects.
Fig. S5. The Bilatre quarry ophicalcites: sample URD12, hand specimen and microscopic aspects.
Fig. S6. In situ U/Pb zircon dating.
Fig. S7. Metasomatic rocks of the crust-mantle detachment.
Fig. S8. Microphotograph of the main rock-types composing the cover décollement fault rocks along (i) the "ball trap" (A to I, location of samples in fig. 10) and (ii) the Peillou sections (J, K, L).
Fig. S9. Triassic tectonic breccia at Peillou: sample BCOR300c.
Fig. S10. Lavas in the Late Albian flysch at Bilatre : macroscopic aspects.
Fig. S11. Lavas in the Late Albian flysch at Bilatre : microscopic aspects.
Table S1. Major and trace element analysis of handpicked glassy spherulites from Bilatre.
Table S2. Operating conditions for the LA-ICP-MS equipment.
Table S3. U-Th-Pb data obtained on zircon grains by LA-ICP-MS.

Table S4. Microprobe mineralogical analyses, sample URD9-1.
Table S5. Microprobe mineralogical analyses, sample URD9b.
Table S6. Microprobe mineralogical analyses, sample URD9c.
Table S7. Microprobe mineralogical analyses, sample URD9f.
Table S8. Microprobe mineralogical analyses, sample BCOR115.
Table S9. Microprobe mineralogical analyses, sample URD17b.
Table S10. Microprobe mineralogical analyses, sample URD17a.
Table S11. Microprobe mineralogical analyses, sample URD16.
Table S12. Microprobe mineralogical analyses, sample URD13.
Table S13. Microprobe mineralogical analyses, sample URD18.
Table S14. Microprobe mineralogical analyses, sample URD14.
Table S15. Microprobe mineralogical analyses, sample URD19.
Table S16. Microprobe mineralogical analyses, sample URD15.
Table S17. Microprobe mineralogical analyses, sample BCOR300a.
Table S18. Microprobe mineralogical analyses, sample BCOR300b.
Table S19. Microprobe mineralogical analyses, sample BCOR300c.
Table S20. Microprobe mineralogical analyses, sample BCOR300e.

The Supplementary Material is available at https://www.bsgf-journal.org/10.1051/bsgf/2019007/olm.

Acknowledgements. This study is the result of 10 years of research in the NPZ and benefited of grants from various programs that are thoroughly acknowledged here. Y.L., P.L. and B.C. were founded by the Référentiel géologique de la France (RGF), BRGM. They are indebted to Thierry Baudin, head of RGF program, for his confidence allowing a 4-year field and laboratory full research period through BC PhD and Master 2 thesis. In addition, Master 2 thesis founds were provided by the RGF program to G. Bergamini and J. Nteme who are thanked here for their contributions. Additional grants were attributed to RA from the OROGEN, INSU/CNRS-BRGM-Total program allowing focus on the Variscan material. ANR Pyramid and ANR Pyrope also provided some funds that were used for fieldwork. We thank Jessica Anglande for assistance at the "microsonde ouest, Plouzané", Joseph Canérot for determination of Urdach microfaunas and Bernard Azambre for his help in microscopic determination of volcanic and metamorphic material. A few persons from the villages nearby Saraillé and Urdach helped our team for lodging and field assistance. In particular, we acknowledge Françoise Pape and Jean-Eric Rose for welcoming us in the Chaînons Béarnais. Y.L. wish to thank especially Loïc Brugalais and Orthofiga, Vern/Seiche, for making fieldwork possible. We thank reviewers Stéphane Guillot, Torgeir Andersen and the associate-editor Romain Augier for their constructive remarks that helped improve our manuscript.

References

Agrinier P, Mével C, Girardeau J. 1988. Hydrothermal alteration of the peridotites cored at the ocean/continent boundary of the Iberian margin: petrologic and stable isotope evidence. In: Boillot G, Winterer EL, *et al.*, eds. *Proceedings of the Ocean Drilling Program, Scientific Results, College Station, TX (Ocean Drilling Program)* 103: 225–234. https://doi.org/10.2973/odp.proc.sr.103.136.1988.

Alt JC, Shanks WC. 2003. Serpentinization of abyssal peridotites from the MARK area, Mid- Atlantic Ridge: sulfur geochemistry and reaction modeling. *Geochim. Cosmochim. Acta* 67: 641–653.

Andersen TB, Corfu F, Labrousse L, Osmundsen PT. 2012. Evidence for hyperextension along the pre-Caledonian margin of Baltica. *Journal of the Geological Society, London* 169: 601–612. DOI: 10.1144/0016-76492012-011.

Andreani M, Mével C, Boullier A, Escartin J. 2007. Dynamic control on serpentine crystallization in veins: constraints on hydration processes in oceanic peridotites. *Geochem. Geophys. Geosystems* 8.

Asti R, Lagabrielle Y, Fourcade S, Corre B, Monié P. (2019). How do continents deform during mantle exhumation? Insights from the northern Iberia inverted paleo-passive margin, western Pyrenees (France). *Tectonics* 38: 1666–1693. DOI: 10.1029/2018TC005428.

Azambre B, Rossy M. 1976. Le magmatisme alcalin d'âge crétacé dans les Pyrénées occidentales; ses relations avec le métamorphisme et la tectonique. *Bulletin de la société Géologique de France* 7(18): 1725–1728.

Azambre B, Rossy M, Albarède F. 1992. Petrology of the alkaline magmatism from the Cretaceous North-Pyrenean Rift Zone (France and Spain). *Eur. J. Mineral.* 4: 813–834.

Bach W, Garrido CJ, Paulick H, Harvey J, Rosner M. 2004. Seawater-peridotite interactions: first insights from ODP Leg 209, MAR 15° N. *Geochemistry Geophysics Geosystems* 5: Q09f26. DOI: 10.1029/2004GC000744.

Beinlich A, Austrheim H, Glodny J, Erambert M, Andersen TB. 2010. CO_2 sequestration and extreme Mg depletion in serpentinized peridotite clasts from the Devonian Solund Basin, SW-Norway. *Geochimica et Cosmochimica Acta* 74: 6935–6964.

Beinlich A, Plümper O, Hövelmann J, Austrheim H, Jamtveit B. 2012. Massive serpentinite carbonation at Linnajavri, N–Norway. *Terra Nova* 24: 446–455. DOI: 10.1111/j.1365-3121.2012.01083.x.

Beslier MO, Royer JY, Girardeau J, Hill PJ, Boeuf E, Buchanan C, *et al.* 2004. Une large transition continent-océan en pied de marges sud-ouest australienne : première résultats de la campagne MARGAU/MD110. *Bulletin de la Société Géologique de France* 175: 629–641.

Biteau JJ, Le Marrec A, Le Vot M, Masset JM. 2006. The Aquitaine Basin. *Petroleum Geoscience* 12(3): 247–273. DOI: 10.1144/1354-079305-674.

Blackman DK, Karson JA, Kelley DS, Cann JR, Früh-Green GL, Gee JS, et al. 2002. Geology of the Atlantis Massif (Mid-Atlantic Ridge, 30 N): implications for the evolution of an ultramafic oceanic core complex. *Mar. Geophys. Res.* 23(866): 443–469.

Boillot G, Recq M, Winterer EL, Meyer AW, Applegate J, Baltuck M, et al. 1987. Tectonic denudation of the upper mantle along passive margins: a model based on drilling results (ODP Leg 103, western Galicia margin, Spain). *Tectonophysics* 132: 335–342.

Boschi C, Fruh-Green GL, Escartin J. 2006a. Occurrence and significance of serpentine-hosted, talc-and amphibole-rich fault rocks in modern oceanic settings and ophiolite complexes: an overview. *Ofioliti* 31(2): 129–140.

Boschi C, Fruh-Green GL, Delacour A, Karson JA, Kelley DS. 2006b. Mass transfer and fluid flow during detachment faulting and development of an oceanic core complex, Atlantis Massif (MAR 30°N). *Geochemistry Geophysics Geosystems* 7: Q01004. DOI: 10.1029/2005GC001074.

Canérot J. 2017a. The pull apart-type Tardets-Mauléon Basin, a key to understand the formation of the Pyrenees. *Bulletin Société géologique de France* 188: 35. DOI: 10.1051/bsgf/2017198.

Canérot J. 2017b. Origine de la chaîne des Pyrénées : collision entre les plaque ibérique et européenne ou inversion d'un ancien rift intracontinental avorté ? *Bull. Soc. Hist. Nat. Toulouse* 153: 95–110.

Canérot J, Delavaux F. 1986. Tectonic and sedimentation on the north Iberian margin, Chainons Béarnais south Pyrenean zone (Pyrenees basco-béarnaises) – New data about the signification of the lherzolites in the Saraillé area. *C. R. Acad. Sci. Ser. II* 302(15): 951–956.

Canérot J, Peybernes B, Cizsak R. 1978. Présence d'une marge méridionale à l'emplacement des Chaînons Béarnais (Pyrénées basco-béarnaises). *Bull. Soc. Geol. Fr.* 7(20): 673–676.

Cannat M, Manatschal G, Sauter D, Peron-Pinvidic G. 2009. Assessing the conditions of continental breakup at magma-poor rifted margins: what can we learn from slow spreading mid-ocean ridges? *C. R. Geoscience.* DOI: 10.1016/j.crte.2009.01.005.

Castanares LM, Robles S, Vicente-Bravo JC. 1997. Distribuciôn estratigrafica de los episodios volcanicos submarinos del Albiense-Santoniense en la Cuenca Vasca (sector Gernika-Plentzia. Bizkaia). *Geogaceta* 22: 43–46.

Castanares LM, Robles S, Gimeno D, Vicente Bravo JC. 2001. The Submarine Volcanic System of the Errigoiti Formation (Albian-Santonian of the Basque-Cantabrian Basin, Northern Spain): Stratigraphic Framework, Facies, and Sequences. *J. Sedim. Res*. 71 (2): 318–333.

Casteras M, Canérot J, Paris J-P., Tisin D, Azambre B, Alimen H. 1970. Carte géol. France (1/50 000), feuille Oloron-Sainte-Marie (1051). Orléans: BRGM.

Chevrot S, Sylvander M, Diaz J, Martin R, Mouthereau F, Manatschal G, *et al.* 2018. The non cylindrical crustal architecture of the Pyrenees. *Scientific Reports* 8: 9591. DOI: 10.1038/s41598-018-27889-x.

Chew DM, van Staal CR. 2014. The ocean-continent transition zones along the Appalachian-Caledonian margin of Laurentia: examples of large-scale hyperextension during the opening of the Iapetus Ocean. *Geoscience Canada* 41: 165–185.

Choukroune P, ECORS team. 1989. The Ecors deep seismic profile reflection data and the overall structure of an orogenic belt. *Tectonics* 8: 23–39.

Choukroune P, Mattauer M. 1978. Tectonique des plaques et Pyrénées : sur le fonctionnement de la faille transformante nord-Pyrénéenne; comparaisons avec les modèles actuels. *Bulletin de la société géologique de France* 20: 689–700.

Clerc C, Lagabrielle Y. 2014. Thermal control on the modes of crustal thinning leading to mantle exhumation: insights from the Cretaceous Pyrenean hot paleomargins. *Tectonics* 33(7): 1340–1359.

Clerc C, Boulvais P, Lagabrielle Y, de Saint Blanquat M. 2014. Ophicalcites from the Northern Pyrenean Belt: a field, petrographic and stable isotope study. *Int. J. Earth Sci*. 103: 141–163. DOI: 10.1007/s00531-013-0927-z.

Clerc C, Lahfid A, Monié P, Lagabrielle Y, Chopin C, Poujol M, *et al.* 2015. High-temperature metamorphism during extreme thinning of the continental crust: a reappraisal of the north Pyrenean passive paleomargin. *Solid Earth* 6: 643–668.

Clerc C, Lagabrielle Y, Labaume P, Ringenbach J-C., Vauchez A, Nalpas T, *et al.* 2016. Basement – Cover decoupling and progressive exhumation of metamorphic sediments at hot-rifted margin. Insights from the Northeastern Pyrenean analog. *Tectonophysics* 686: 82–97.

Corre B, Lagabrielle Y, Labaume P, Fourcade S, Clerc C, Ballèvre M. 2016. Deformation associated with mantle exhumation in a distal, hot passive margin environment: new constraints from the Saraillé Massif (Chaînons Béarnais, North-Pyrenean Zone). *Compt. Rendus Geosci.* 348: 279–289.

Corre B, Boulvais P, Boiron MC, Lagabrielle Y, Marasi L, Clerc C. 2018. Fluid circulations in response to mantle exhumation at the passive margin setting in the north Pyrenean zone, France. *Mineralogy and Petrology.* DOI: 10.1007/s00710-018-0559-x.

Corre B. 2017. La bordure nord de la plaque ibérique à l'Albo-Cénomanien. Architecture d'une marge passive de type ductile. Chaînons Béarnais, Pyrénées occidentales: Unpublished thesis, Univ. Rennes 1, 300 p.

Debroas E-J. 1978. Évolution de la fosse du flysch ardoisier de l'Albien supérieur au Sénonien inférieur (zone interne métamorphique des Pyrénées navarro-languedociennes). *Bull. Soc. Géol. Fr.* 20: 639–648.

Debroas EJ, Canérot J, Bilotte M. 2010. Les Brèches d'Urdach, témoins de l'exhumation du manteau pyrénéen dans un escarpement de faille Vraconnien-Cénomanien inférieur (zone nord-pyrénéenne, Pyrénées-Atlantiques, France). *Géol. Fr.* 2: 53–63.

DeFelipe I, Pedreira D, Pulgar JA, Iriarte E, Mendia M. 2017. Mantle exhumation and metamorphism in the Basque-Cantabrian Basin (N Spain): stable and clumped isotope analysis in carbonates and comparison with ophicalcites in the North-Pyrenean Zone (Urdach and Lherz). *Geochem. Geophys. Geosyst.* 18(2): 631–652.

Delacour A, Früh-Green GL, Bernasconi SM. 2008a. Sulfur mineralogy and geochemistry of serpentinites and gabbros of the Atlantis Massif (IODP Site U1309). *Geochimica et Cosmochimica Acta*. 72: 5111–5127. DOI: 10.1016/j.gca.2008.07.018.

Delacour A, Früh-Green GL, Frank M, Gutjahr M, Kelley DS. 2008b. Sr- and Nd-isotope geochemistry of the Atlantis Massif (30°N, MAR): Implications for fluid fluxes and lithospheric heterogeneity. *Chem. Geol*. 254: 19–35. DOI: 10.1016/j.chemgeo.2008.05.018.

Denny AR, Kelley DS, Früh-Green GL. 2015. Geologic evolution of the Lost City Hydrothermal Field. *Geochem. Geophys. Geosyst*. 17: 375–394. DOI: 10.1002/2015GC005869.

Duée G, Lagabrielle Y, Coutelle A, Fortané A. 1984. Les lherzolites associées aux chaînons béarnais (Pyrénées Occidentales) : mise à l'affleurement anté-dogger et resédimentation albo-cénomanienne. *C.R. Acad. Sci., Paris*, t. 299(série II, n° 17): 1205–1209.

Escartin J, Hirth G, Evans B. 1997. Effects of serpentinization on the lithospheric strength and the style of normal faulting at slow-spreading ridges. *Earth and Planetary Science Letters* 181–189.

Escartín J, Mével C, MacLeod CJ, McCaig AM. 2003. Constraints on deformation conditions and the origin of oceanic detachments: the Mid-Atlantic Ridge core complex at 15°45'N. *Geochemistry, Geophys. Geosystems* 4: 1067. DOI: 10.1029/2001GC000278.

Escartin J, Smith DK, Cann J, Schouten H, Langmuir CH, Escrig S. 2008. Central role of detachment faults in accretion of slow-spreading oceanic lithosphere. *Nature* 455: 790–794.

Escartín J, Mével C, Petersen S, Bonnemains D, Cannat M, Andreani M, *et al.* 2017. Tectonic structure, evolution, and the nature of oceanic core complexes and their detachment fault zones (13°20'N and 13°30'N, Mid Atlantic Ridge). *Geochem. Geophys. Geosys*. 18 (4): 1451–1482. DOI: 10.1002/2016GC006775.

Fabriès J, Lorand J-P, Bodinier J-L, Dupuy C. 1991. Evolution of the upper mantle beneath the Pyrenees: evidence from orogenic spinel

lherzolite massifs. *J. Petrol., sp. volume "Orogenic lherzolites and mantle processes"* 55–76.
Fabriès J, Lorand J-P., Bodinier J-L. 1998. Petrogenetic evolution of orogenic lherzolite massifs in the central and western Pyrenees. *Tectonophysics* 292: 145–167.
Fallourd S, Poujol M, Boulvais P, Paquette JL, de Saint Blanquat M, Rémy P. 2014. In situ LA-ICP-MS U–Pb titanite dating of Na–Ca metasomatism in orogenic belts: the North Pyrenean example. *Int J Earth Sci* 103(3): 667–682.
Fortané A, Duée G, Lagabrielle Y, Coutelle A. 1986. Lherzolites and the Western ''Chaînons Béarnais'' (French Pyrénées): structural and paleogeographical pattern. *Tectonophysics* 129: 81–98.
Früh-Green GL, Kelley DS, Bernasconi SM, Karson JA, Ludwig KA, Butterfield DA, *et al.* 2003. 30,000 years of hydrothermal activity at the Lost City vent field. *Science* 301: 495–498.
Gaudichet A. 1974. Étude pétrographique des lherzolites de la région d'Oloron-Ste Marie (Pyrénées Atlantiques). Unpublished Thesis, University of Paris VI.
Gillard M, Autin J, Manatschal G, Sauter D, Munschy M, Schaming M. 2015. Tectonomagmatic evolution of the final stages of rifting along the deep conjugate Australian-Antarctic magma-poor rifted margins: constraints from seismic observations. *Tectonics* 34: 753–783. DOI: 10.1002/2015tc003850.
Golberg J-M, Leyreloup A-F. 1990. High temperature-low pressure Cretaceous metamorphism related to crustal thinning (Eastern North Pyrenean Zone, France). *Contributions to Mineralogy and Petrology* 104(2): 194–207. DOI: 10.1007/BF00306443.
Halls C, Zhao R. 1995. Listvenite and related rocks: perspectives on terminology and mineralogy with reference to an occurrence at Cregganbaun, Co. Mtayo, Republic of Ireland. *Miner. Deposita* 30: 303–313.
Harlov DE, Austrheim H. 2013. *Metasomatism and the chemical transformation of rocks. The role of fluids in terrestrial and extraterrestrial processes. Lecture notes in Earth Sciences*. Berlin Heidelberg: Springer-Verlag, 806 p. DOI: 10.1007/978-3-642-28394-9.
Jakob J, Andersen TB, Kjøll HJ. 2019. A review and revision of the rift – inherited architecture of the South and Central Scandinavian Caledonides – a magma-poor to magma-rich transition and the significance of reactivation of rift-inheritance during the Caledonian Orogeny. *Earth Science Review*. DOI: 10.1016/j.earscirev.2019.01.004.
Jammes S, Manatschal G, Lavier LL, Masini E. 2009. Tectonosedimentary evolution related to extreme crustal thinning ahead of a propagating ocean: example of the western Pyrenees. *Tectonics* 28 (4). DOI: 10.1029/2008TC002406.
Karson J, Früh-Green G, Kelley DS, Williams E, Yoerger DR, Jakuba M. 2006. Detachment shear zone of the Atlantis Massif core complex, Mid-Atlantic Ridge, 30 N. *Geochem. Geophys. Geosystems* 7.
Kelemen P, Matter J, Streit L, Rudge J, Curry B, Blusztajn J. 2011. Rates and mechanism of mineral carbonation in peridotite: natural processes and recipes for enhanced, in situ CO_2 capture and storage. *Annual Review of Earth and Planetary Sciences*. DOI: 10.1146/annurev-earth-092010-152509.
Lafay R, Baumgartner PL, Schwartz S, Picazo S, Montes-Hernandez G, Torsten V. 2017. Petrologic and stable isotopic studies of a fossil hydrothermal system in ultramafic environment (Chenaillet ophicalcites, Western Alps, France): processes of carbonate cementation. *Lithos V.* 294-295, 319–338. DOI: 10.1016/j.lithos.2017.10.006.
Lagabrielle Y, Bodinier JL. 2008. Submarine reworking of exhumed subcontinental mantle rocks: field evidence from the Lherz peridotites, French Pyrenees. *Terra Nova* 20(1): 11–21. DOI: 10.1111/j.1365-3121.2007.00781.
Lagabrielle Y, Labaume P, de Saint Blanquat M. 2010. Mantle exhumation, crustal denudation, and gravity tectonics during Cretaceous rifting in the Pyrenean realm (SW Europe): insights from the geological setting of the lherzolite bodies. *Tectonics* 29(4).
Lagabrielle Y, Clerc C, Vauchez A, Lahfid A, Labaume P, Azambre B, *et al.* 2016. Very high geothermal gradient during mantle exhumation recorded in mylonitic marbles and carbonate breccias from a Mesozoic Pyrenean palaeomargin (Lherz area, North Pyrenean Zone, France). *Compt. Rendus Geosci.* 348: 257–267.
Lagabrielle Y, Asti R, Fourcade S, Corre B, Uzel J, Labaume P, *et al.* (2019). Mantle exhumation at magma-poor passive continental margins. Part II. Tectonic and metasomatic evolution of large-displacement detachment faults preserved in a fossil distal margin domain (Saraillé lherzolites, north-western Pyrenees, France). *Geosciences Bulletin BSGF*. (in press).
Larsen HC, Mohn G, Nirrengarten M, *et al.* 2018. Rapid transition from continental breakup to igneous oceanic crust in the South China Sea. *Nature Geoscience* 11(10). DOI: 10.1038/s41561-018-0198-1.
Le Pichon X, Bonnin J, Sibuet JC. 1970. La faille nord-pyrénéenne : faille transformante liée à l'ouverture du Golfe de Gascogne. *C.R. Acad. Sc. Paris* 271(série D): 1941–1944.
Lemoine M. 1980. Serpentinites, gabbros and ophicalcites in the Piemont-Ligurian domain of the Western Alps: possible indicators of oceanic fracture zones and of associated serpentinite protrusions in the Jurassic-Cretaceous Tethys. *Arch Sci* 33: 103–115.
Lemoine M, Tricart P, Boillot G. 1987. Ultramafic and gabbroic ocean floor of the Ligurian Tethys (Alps, Corsica, Apennines): In search of a genetic imodel. *Geology* 15: 622–625.
Ludwig KA, Kelley DS, Butterfield DA, Nelson BK, Früh-Green G. 2006. Formation and evolution of carbonate chimneys at the Lost City Hydrothermal Field. *Geochim. Cosmochim. Acta* 70: 3625–3645.
Luhr JF, Aranda-Gomez JJ, Housh TB. 1995. San Quintin volcanic field, Baja California Norte, Mexico: geology, petrology and geochemistry. *J. Geophys. Res.* 100: 10353–10380.
Machel HG. 2001. Bacterial and thermochemical sulfate reduction in diagenetic settings – old and new insights. *Sedimentary Geology* 140: 143–175.
MacLeod CJ, Escartin J, Banerji D, Banks GJ, Gleeson M, Irving DHB, *et al.* 2002. Direct geological evidence for oceanic detachment faulting: the Mid-Atlanic Ridge, 15°45'N. *Geology* 30: 879–882.
Manatschal G, Nievergelt P. 1997. A continent-ocean transition recorded in the Err and Platta nappes (eastern Switzerland). *Eclogae Geol. Helv.* 90: 3–27.
Manatschal G. 2004. New models for evolution of magma-poor rifted margins based on a review of data and concepts from West Iberia and the Alps. *Int. J. Earth Sci.* 93: 432–466.
Marroni M, Pandolfi L. 2007. The architecture of an incipient oceanic basin: a tentative reconstruction of the Jurassic Liguria-Piemonte basin along the Northern Apennines – Alpine Corsica transect. *International Journal of Earth Sciences* 96: 1059–1078.
Masini E, Manatschal G, Tugend J, Mohn G, Flament JM. 2014. The tectono-sedimentary evolution of a hyper-extended rift basin: the example of the Arzacq–Mauléon rift system (Western Pyrenees, SW France). *Int. J. Earth Sci*. 1–28. DOI: 10.1007/s00531-014-1023-8.
Menzel MD, Garrido CJ, Lopez Sanchez-Vizcaino V, Marchesi C, Hidas K, Escayola MP, *et al.* 2018. Carbonation of mantle peridotite by CO_2-rich fluids: the formation of listvenites in the Advocate ophiolite complex. Newfoundland, Canada: Lithos. DOI: 10.1016/j.lithos.2018.06.001.

Mével C. 2003. Serpentinization of abyssal peridotites at mid-ocean ridges. *Comptes Rendus Geosci.* 335: 825–852. DOI: 10.1016/j.crte.2003.08.006.

Mohn G, Manatschal G, Beltrando M, Masini E, Kusznir N. 2012. Necking of continental crust in magma-poor rifted margins: evidence from the fossil Alpine Tethys margins. *Tectonics* 31: TC1012. DOI: 10.1029/2011TC002961.

Monchoux P. 1970. *Les lherzolites pyrénéennes. Contribution à l'étude de leur minéralogie, de leur genèse et de leurs transformations. Thèse d'état*. Toulouse, 180 p.

Monchoux P, Fontan F, De Parseval P, Martin RF, Wang RC. 2006. Igneous albitite dikes in orogenic lherzolites, western Pyrénées, France: a possible source for corundum and alkali feldspar xenocrysts in basaltic terranes. I. Mineralogical associations. *Can Mineral.* 44: 811–836.

Montigny R, Azambre B, Rossy M, Thuizat R. 1986. K-Ar study of Cretaceous magmatism and metamorphism in the Pyrénées: age and length of rotation of the Iberian peninsula. *Tectonophysics* 129: 257–273.

Mouthereau F, Filleaudeau PY, Vacherat A, Pik R, Lacombe O, Fellin MG, *et al.* 2014. Placing limits to shortening evolution in the Pyrenees: role of margin architecture and implications for the Iberia/Europe convergence. *Tectonics* 33: 2283–2314. DOI: 10.1002/2014TC003663.

Muñoz JA. 1992. Evolution of a continental collision belt: ECORS-Pyrenees crustal balanced cross-section. In: McClay KR, ed. *Thrust tectonics*. London, UK: Chapman and Hall, pp. 235–246.

Nteme J. 2017 Interactions fluides/roches durant l'exhumation du manteau. Étude des inclusions fluides dans un détachement majeur de la zone nord-Pyrénéenne (Urdach : Chaînons Béarnais). Unpublished Master 2 thesis. Géosciences. Rennes, France: 24 p.

Olivet JL. 1996. La cinématique de la plaque ibérique. *Bull. Cent. Rech. Explor. Prod. Elf Aquitaine* 20(1): 131–195.

Pérez-Gussinyé M, Phipps-Morgan J, Reston TJ, Ranero CR. 2006. From rifting to spreading at nonvolcanic margins: insights form numerical modeling. *Earth and Planetary Science Letters* 244: 458–473.

Pérez-Gussinyé. 2013. A tectonic model for hyperextension at magma-poor rifted margins: an example from the West Iberia – Newfoundland conjugate margins. In : Mohriak WU, Danforth A, Post PJ, Brown DE, Tari GC, Nemčok M, Sinha ST, eds. *Conjugate divergent margins*. Geological Society, London: Special Publications, 369, pp. 403–427.

Péron-Pinvidic G, Manatschal G. 2009. The final rifting evolution at deep magma-poor passive margins from Iberia-Newfoundland: a new point of view. *International Journal of Earth Sciences* 98(7): 1581–1597.

Péron-Pinvidic G, Osmundsen PT. 2016. Architecture of the distal and outer domains of the mid-Norwegian Vøring rifted margin: insights from the Rån Ridge system. *Mar. Petrol. Geol.* 77: 280–299.

Picazo S, Cannat M, Delacour A, Escartín J, Rouméjon S, Silantyev S. 2012. Deformation associated with the denudation of mantle-derived rocks at the Mid-Atlantic Ridge 13°-15° N: the role of magmatic injections and hydrothermal alteration. *Geochem. Geophys. Geosystems* 13.

Pin C, Paquette J-L., Monchoux P, Hammouda T. 2001. First field-scale occurrence of Si-Al-Na-rich low-degree partial melt from the upper mantle. *Geology* 29: 451–454.

Pin C, Monchoux P, Paquette J-L., Azambre B, Wang RC, Martin RF. 2006. Igneous albitite dikes in orogenic lherzolites, Western Pyrénées, France: a possible source for corundum and alkali feldspar xenocrysts in basaltic terranes. II. Geochemical and petrogenetic considerations. *Canad. Mineral.* 44: 843–856.

Pinto VHG, Manatschal G, Karpoffv AM, Viana A. 2015. Tracing mantle-reacted fluids in magma-poor rifted margins: the example of Alpine Tethyan rifted margins. *Geochem. Geophys. Geosyst.* 16. DOI: 10.1002/2015GC005830.

Plissart G, Féménias O, Maruntiu M, Diot H, Demaiffe D. 2009. Mineralogy and geothermometry of gabbro-derived listvenites in the Tosovita-Iuti ophiolite, southwestern Romania. *The Canadian Mineralogist* 47: 81–105. DOI: 10.3749/canmin.47.1.81.

Poujol M, Boulvais P, Kosler J. 2010. Regional-scale Cretaceous albitization in the Pyrenees: evidence from in situ U-Th-Pb dating of monazite, titanite and zircon. *J Geol Soc* 167(4): 751–767.

Reston TJ. 2009a. The extension discrepancy and syn-rift subsidence deficit at rifted margins. *Petroleum Geoscience* 15: 217–237. DOI: 10.1144/1354-079309-845.

Reston TJ. 2009b. The structure, evolution and symmetry of the magma-poor rifted margins of the North and Central Atlantic: a Synthesis. *Tectonophysics* 468: 6–27.

Rodriguez Garcia D, Villanova-de-Benavent C, Butjosa L, Aiglesperger T, Melgarejo JC, Proenza JA, *et al.* 2015. *Au Mineralisation in "Listvenites" from Mina Descanso, Central Cuba: preliminary results. Geodynamics, Orogenic cycles and mineral systems. Mineral resources in a sustainable world*, 13th SGA Biennial Meeting 2015. Proceedings, V. 1, Conference Paper, August 2015.

Roure F, Choukroune P. 1998. Contribution of the Ecors seismic data to the Pyrenean geology: crustal architecture and geodynamic evolution of the Pyrenees. *Mémoires de la Société géologique de France* 173: 37–52.

Roure F, Choukroune P, Berastegui X, Munoz JA, Vilien A, Matheron P, et al. 1989. Ecors deep seismic data and balanced cross sections: geometric constraints on the evolution of the Pyrenees. *Tectonics* 8: 41–50.

Roux JC. 1983. Recherches stratigraphiques et sédimentologiques sur les flysch crétacés pyrénéens au Sud d'Oloron (Pyrénées Atlantiques). Toulouse: Thèse 3ème cycle, Université Paul Sabatier.

Saint Blanquat de M, Bajolet F, Grand'Homme A, Proietti A, Zanti M, Boutin A, *et al.* 2016. Cretaceous mantle exhumation in the central Pyrenees: new constraints from the peridotites in eastern Ariège (North Pyrenean zone, France). *Compt. Rendus Geosci.* 348: 268–278.

Schärer U, de Parseval P, Polvé M, St Blanquat M. 1999. Formation of the Trimouns talc-chlorite deposit (Pyrenees) from persistent hydrothermal activity between 112 and 97 Ma. *Terra Nova* 11(1): 30–37. DOI: 10.1046/j.13653121.1999.00224.x.

Schoeffler J, Henry J, Villanova M. 1964. État des travaux de cartographie géologique réalisés par la Société nationale des pétroles d'Aquitaine (SNPA) dans les Pyrénées occidentales. *C. R. somm. Soc. géol. Fr.* 7: 241–246.

Schroeder T, John B, Frost BR. 2002. Geologic implications of seawater circulation through 1116 peridotite exposed at slow-spreading mid-ocean ridges. *Geology* 30: 367–370. 1117. DOI: 10.1130/0091-7613(2002)030<0367:GIOSCT>2.0.CO;2.

Sibuet JC, Srivastava SP, Spakman W. 2004. Pyrenean orogeny and plate kinematics. *Journal of Geophysical Research, Washington* 109: B08104. DOI: 10.1029/2003JB002514. 18 p.

Soto JI, Flinch JF, Tari G. 2017. Permo-Triassic salt provinces of Europe, North Africa and the Atlantic margins: a synthesis. In : Soto *et al.*, eds. *Permo-Triassic salt provinces of Europe, North Africa and the Atlantic margins. Tectonics and Hydrocarbon potential*. Elsevier, pp. 3–41.

Sutra E, Manatschal G, Mohn G, Unternehr P. 2013. Quantification and restoration of extensional deformation along the Western Iberia and Newfoundland rifted margins. *Geochem. Geophys. Geosyst*. 14 (8): 2575–2597. DOI: 10.1002/ggge.20135.

Teixell A. 1998. Crustal structure and orogenic material budget in the west central Pyrenees. *Tectonics* 17(3): 395–406.

Teixell A, Labaume P, Lagabrielle Y. 2016. The crustal evolution of the west-central Pyrenees revisited: inferences from a new kinematic scenario. *Comptes Rendus Geoscience* 348, 257, 267. DOI: 10.1016/j.crte.2015.10.010.

Teixell A, Labaume P, Ayarza P, Espurt N, de Saint Blanquat M, Lagabrielle Y. 2018. The present-day and past crustal structure of the Pyrenean-Cantabrian belt: a review and new interpretations from recent concepts and data. *Tectonophysics* DOI: 10.1016/j.tecto.2018.01.009.

Thiébault J, Durand-Wackenheim C, Debeaux M, Souquet P. 1992. Métamorphisme des évaporites triasiques du versant nord des Pyrénées centrales et occidentales. *Bull Soc Hist Nat Toulouse* 128: 77–84.

Trommsdorff V, Evans BW, Pfeifer H. 1980. Ophicarbonate rocks: metamorphic reactions and possible origin. *Arch Sci Geneve* 33: 3610364.

Treves BE, Harper GD. 1994. Exposure of serpentinites on the ocean floor: sequence of faulting and hydrofracturing in the northern Apennine ophicalcites. *Ofioliti* 19b: 435–466.

Tucholke BE, Sibuet J-C, Klaus A, eds. 2007. Proc. ODP, Sci. Results, 210: College Station, TX (Ocean Drilling Program). DOI: 10.2973/odp.proc.sr.210.2007.

Tugend J, Manatschal G, Kusznir NJ, Masini E, Mohn G, Thinon I. 2014. Formation and deformation of hyperextended rift systems: insights from rift domain mapping in the Bay of Biscay-Pyrenees. *Tectonics* 33. DOI: 10.1002/2014TC003529.

Vergés J, Garcia-Senz J. 2001. Mesozoic evolution and Cainozoic inversion of the Pyrenean rift. In : Ziegler PA, Cavazza W, Robertson AHF, Crasquin-Soleau S, eds. *Peri-Tethys Memoir 6: Peri-Tethyan Rift/Wrench Basins and Passive margins*. Mémoires du Muséum Nationale d'Histoire Naturelle, 186, pp. 187–212.

Vergés J, Millán H, Muñoz JA, Marzo M, Cirès J, Den Bezemer T, *et al.* 1995. Eastern Pyrenees and related foreland basins: pre-, syn- and post-collisional crustal-scale cross-sections. *Marine and Petroleum Geology* 12(8): 893–915.

Vielzeuf D, Kornprobst J. 1984. Crustal splitting and the emplacement of Pyrenean lherzolites and granulites. *Earth Planet. Sci. Lett.* 67: 87–96.

Vissers RLM, Meijer PT. 2012. Mesozoic rotation of Iberia: subduction in the Pyrenees? *Earth Sci Rev* 110(1–4): 93–110. DOI: 10.1016/j.earscirev.2011.11.001.

Wilson M. 1989. *Igneous petrogenesis. A global tectonic approach*. London: Chapman and Hall, 466 p.

Wilson M, Downes H. 1992. Mafic alkali volcanism associated with the European Cenozoic rift system. *Tectonophysics* 208: 173–182.

Wrobel-Daveau J-C, Ringenbach J-C, Tavakoli S, Ruiz GMH, Masse P, Frizon de Lamotte D. 2010. Evidence for mantle exhumation along the Arabian marginin the Zagros (Kermanshah area, Iran). *Arabian Journal of Geosciences* 3(4): 499–513. DOI: 10.1007/s12517-010-0209-z.

Cite this article as: Lagabrielle Y, Asti R, Fourcade S, Corre B, Poujol M, Uzel J, Labaume P, Clerc C, Lafay R, Picazo S, Maury R. 2019. Mantle exhumation at magma-poor passive continental margins. Part I. 3D architecture and metasomatic evolution of a fossil exhumed mantle domain (Urdach lherzolite, north-western Pyrenees, France), *BSGF - Earth Sciences Bulletin* 190: 8.